

# Engineering Complex Orthopaedic Tissues *Via* Strategic Biomimicry

DOVINA QU, CHRISTOPHER Z. MOSHER, MARGARET K. BOUSHELL, and HELEN H. LU

Biomaterials and Interface Tissue Engineering Laboratory, Department of Biomedical Engineering, Columbia University, 1210 Amsterdam Avenue, 351 Engineering Terrace, MC 8904, New York, NY 10027, USA

(Received 3 July 2014; accepted 13 November 2014; published online 3 December 2014)

Associate Editor Fei Wang oversaw the review of this article.

**Abstract**—The primary current challenge in regenerative engineering resides in the simultaneous formation of more than one type of tissue, as well as their functional assembly into complex tissues or organ systems. Tissue–tissue synchrony is especially important in the musculoskeletal system, wherein overall organ function is enabled by the seamless integration of bone with soft tissues such as ligament, tendon, or cartilage, as well as the integration of muscle with tendon. Therefore, *in lieu* of a traditional single-tissue system (e.g., bone, ligament), composite tissue scaffold designs for the regeneration of functional connective tissue units (e.g., *bone–ligament–bone*) are being actively investigated. Closely related is the effort to re-establish tissue–tissue interfaces, which is essential for joining these tissue building blocks and facilitating host integration. Much of the research at the forefront of the field has centered on bioinspired stratified or gradient scaffold designs which aim to recapitulate the structural and compositional inhomogeneity inherent across distinct tissue regions. As such, given the complexity of these musculoskeletal tissue units, the key question is how to identify the most relevant parameters for recapitulating the native structure–function relationships in the scaffold design. Therefore, the focus of this review, in addition to presenting the state-of-the-art in complex scaffold design, is to explore how *strategic biomimicry* can be applied in engineering tissue connectivity. The objective of *strategic biomimicry* is to avoid over-engineering by establishing what needs to be learned from nature and defining the essential matrix characteristics that must be reproduced in scaffold design. Application of this engineering strategy for the regeneration of the most common musculoskeletal tissue units (e.g., *bone–ligament–bone*, *muscle–tendon–bone*, *cartilage–bone*) will be discussed in this review. It is anticipated that these exciting efforts will enable integrative and functional

repair of soft tissue injuries, and moreover, lay the foundation for the development of composite tissue systems and ultimately, total limb or joint regeneration.

**Keywords**—Scaffolds, Interface, Tissue engineering, Complex tissues, Strategic biomimicry.

## INTRODUCTION

The prevalence of trauma and disease resulting in the loss or failure of tissue and organ function has engendered an unmet clinical need for the development of strategies to repair and regenerate damaged tissues. Combining biomaterials, cells, as well as chemical and physical cues, tissue engineering principles<sup>59,107</sup> have been successfully applied in recent years to form a variety of single-tissue systems both *in vitro* and *in vivo*. From a structure–function perspective, the organs of the body are comprised of diverse tissue types which interface with each other and operate in synchrony to enable complex functions. Therefore, to recapitulate native biological function, the next horizon in the field of tissue engineering resides in how to assemble these single-tissue systems into multi-tissue units or facilitate the integration of these composite tissue grafts *in vivo*.

Synchronized tissue units are especially important in the musculoskeletal system, wherein physiologic motion is orchestrated through well-organized and concerted actions of bone in conjunction with a variety of soft tissues, including, *ligaments*, which connect bone to bone, *tendons*, which join muscle to bone, and *cartilage*, which lines the surface of articulating joints. The tissue–tissue junctions through which they integrate with each other are characterized by multiple tissue regions that exhibit well-defined, spatial changes in cell phenotype, matrix composition and organization, as well as region-specific mechanical properties (Fig. 1).

Address correspondence to Helen H. Lu, Biomaterials and Interface Tissue Engineering Laboratory, Department of Biomedical Engineering, Columbia University, 1210 Amsterdam Avenue, 351 Engineering Terrace, MC 8904, New York, NY 10027, USA. Electronic mail: hllu@columbia.edu

Unfortunately, these connective junctions are also prone to injury and degeneration, and are not reestablished *via* standard surgical repair methods. For example, in the majority of anterior cruciate ligament (ACL) injuries, a relatively homogenous tendon graft is used to replace the damaged ligament and is fixed within the bone tunnel with pins or screws. However, this single-tissue oriented strategy does not facilitate regeneration of the functional soft-hard tissue unit of the native ACL. Instead disorganized fibrovascular tissue is formed within the bone tunnel,<sup>93</sup> resulting in a structurally weak link between graft and bone that is often susceptible to failure, leading to poor long-term outcomes and reduced mobility for the patient.<sup>35</sup> Similarly, repair methods for rotator cuff tears can be associated with post-surgical failure rates as high as 94%.<sup>31</sup> The prevalence of osteoarthritis, especially among the aging population, has further increased the demand for soft tissue repair therapies as current cartilage treatment options are similarly limited by poor integration of grafted tissue with the underlying bone and host cartilage.<sup>44</sup> It is clear that there exists an unmet clinical need for functional and integrative treatment strategies for the repair of orthopaedic soft tissue injuries.

While a number of approaches to musculoskeletal soft tissue regeneration have been explored with promising results,<sup>46,61,120,125</sup> successful clinical translation of these grafts will depend largely on how best to achieve functional and extended integration of the engineered tissue units with each other and the surrounding host tissue. The inherent complexity and structural intricacy of the native junction between soft and hard tissues underscore the difficulties in engineering tissue–tissue interfaces. Each tissue phase is characterized as having distinct cellular populations and unique matrix composition and organization, yet must operate in unison with adjoining tissues to facilitate physiologic function and maintain tissue homeostasis. Inspired by these multi-tissue structures, a variety of complex scaffold designs seeking to recapitulate the native spatial and compositional inhomogeneity have been developed.<sup>4,28,77</sup> This review will discuss current regenerative engineering efforts in ligament–bone<sup>3,11,19,21,54,62,68,71,72,86,87,96–98,110,111,113–115</sup> tendon–bone,<sup>24,78,79,134</sup> muscle–tendon,<sup>57,58,60,117,118</sup> and cartilage–bone integration<sup>1,5,13,15–18,25–27,30,32,33,36,37,39,41,47,49,52,53,55,56,69,74,92,95,100–104,106,119,128,133,135–137</sup> focusing on biomaterial- and cell-based strategies for engineering biomimetic, functional spatial variations in composition and mechanical properties. In light of the complexity of multi-tissue regeneration, the application of *strategic biomimicry* across tissue–tissue junctions, or prioritizing what needs to be recapitulated from native tissues and identifying the most crucial parameters for complex scaffold design, is

essential for avoiding over-engineering the scaffold system. This review will highlight these strategic design approaches and conclude with a summary and reflections on future directions in complex tissue engineering.

## COMPLEX SCAFFOLD DESIGN FOR INTEGRATIVE LIGAMENT TISSUE ENGINEERING

Anatomically, ligaments are anchored to bone either through fibrous insertions, wherein aligned collagen fibers connect the soft tissue to the periosteum,<sup>90</sup> or through direct insertions *via* a two-region fibrocartilaginous interface.<sup>130</sup> In other words, the functional ligament is a multi-tissue unit which consists of several compositionally distinct and structurally continuous regions: *bone–interface–ligament–interface–bone*. For example, the ACL, which is the primary stabilizer of the knee joint, spans from femur to tibia and joins to each bony end *via* a fibrocartilaginous insertion (Fig. 1). The fibrocartilage interface is further subdivided into mineralized and non-mineralized regions, with an exponential increase in mineral content observed within the calcified region.<sup>109</sup> A structurally and/or compositionally heterogeneous scaffold design is therefore necessary to recapitulate the composite tissue structure across the ligament–bone junction.

Ideally, such a scaffold should exhibit phase-specific mechanical properties which increase from the ligament to bone phase and exhibit mechanical competence under physiologic tension and torsion. Additionally the scaffold must support the growth and differentiation of relevant cell populations, facilitate their interactions, promote and maintain controlled matrix heterogeneity, and be biodegradable in order to be gradually replaced by newly generated tissue. Specifically, the neoligament tissue should exhibit organized matrix comprised predominantly of collagen I and III, while fibrocartilaginous tissue is characterized by a matrix consisting of glycosaminoglycans (GAG) in collagens I and II, and bone exhibits a mineralized, collagen I matrix. Complex scaffolds for multi-tissue regeneration must not only facilitate regeneration of each discrete tissue type of interest, but also achieve integration of these multiple tissue phases. To this end, interconnectivity and integration of adjacent phases, as well as adaptability and compatibility with current surgical repair methods, are associated requirements in scaffold design and fabrication.

While traditional efforts to develop tissue-engineered ACL grafts have predominantly focused on the ligament proper,<sup>125,129</sup> there has been a recent shift towards forming multi-tissue units consisting of inte-

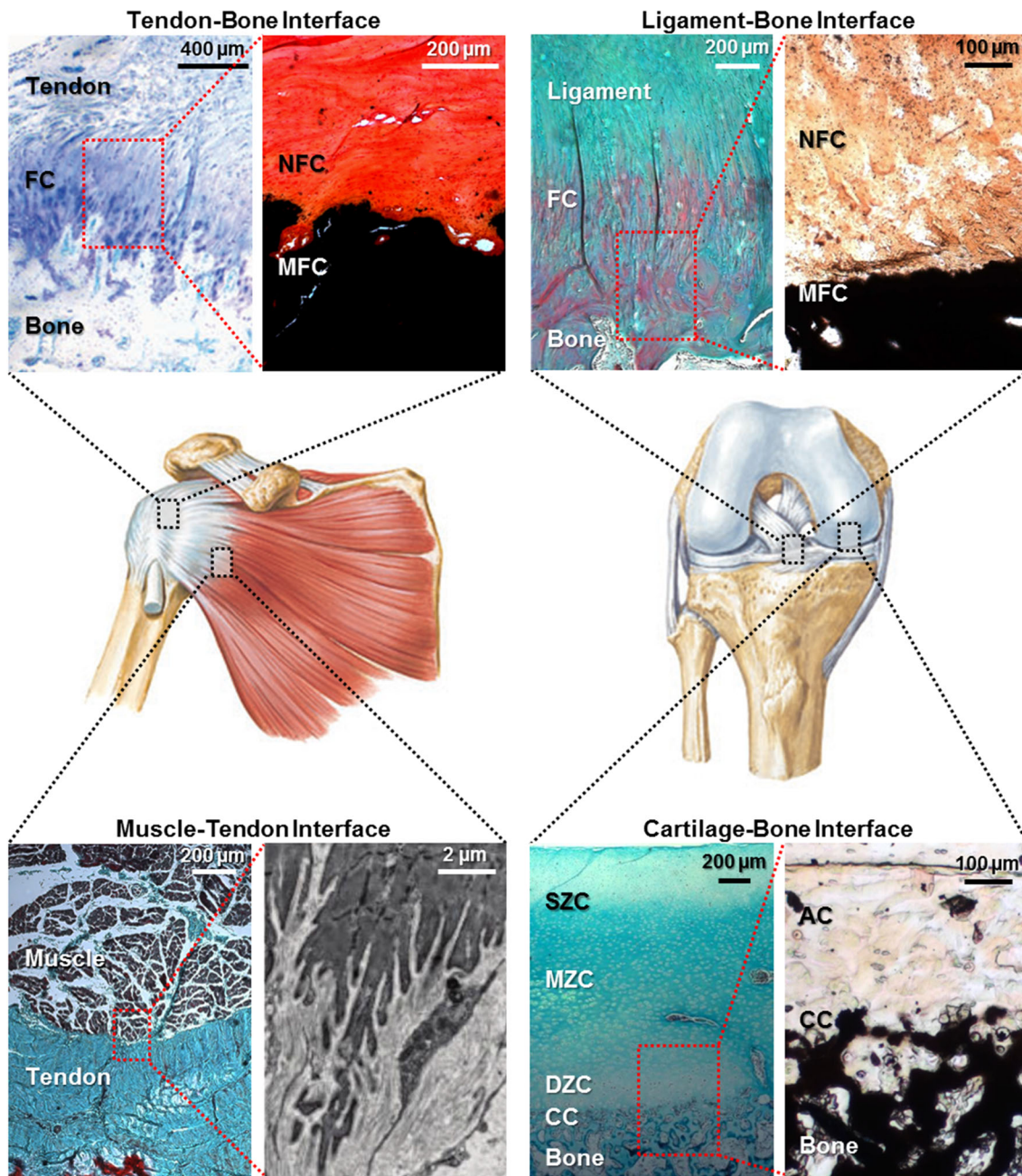


**FIGURE 1.** Common orthopaedic tissue-tissue interfaces. Ligaments, such as the anterior cruciate ligament (ACL) in the knee (Modified Goldner's Masson Trichrome),<sup>126</sup> and tendons, such as the supraspinatus tendon in the shoulder (Toluidine blue),<sup>70</sup> connect to bone via a fibrocartilaginous (FC) transition, which can be further subdivided into non-mineralized (NFC) and mineralized (MFC) regions (Von Kossa). The muscle-tendon junction (Modified Goldner's Masson Trichrome) consists of an interdigitating band of connective tissue.<sup>60</sup> Articular cartilage (AC), which can be subdivided into surface (SZC), middle (MZC), and deep (DZC) zones (Modified Goldner's Masson Trichrome), connects to subchondral bone via a transitional calcified cartilage (CC) region (Von Kossa).

grated *bone-ligament-bone*, *ligament-bone* or *ligament-interface-bone* regions (Table 1). For *bone-ligament-bone* designs, Bourke *et al.* first reported a scaffold consisting of polydesamino tyrosyl-tyrosine ethyl ester carbonate or polylactide (PLA) fibers embedded in polymethyl methacrylate plugs.<sup>11</sup> Improving upon this design concept, Cooper *et al.*

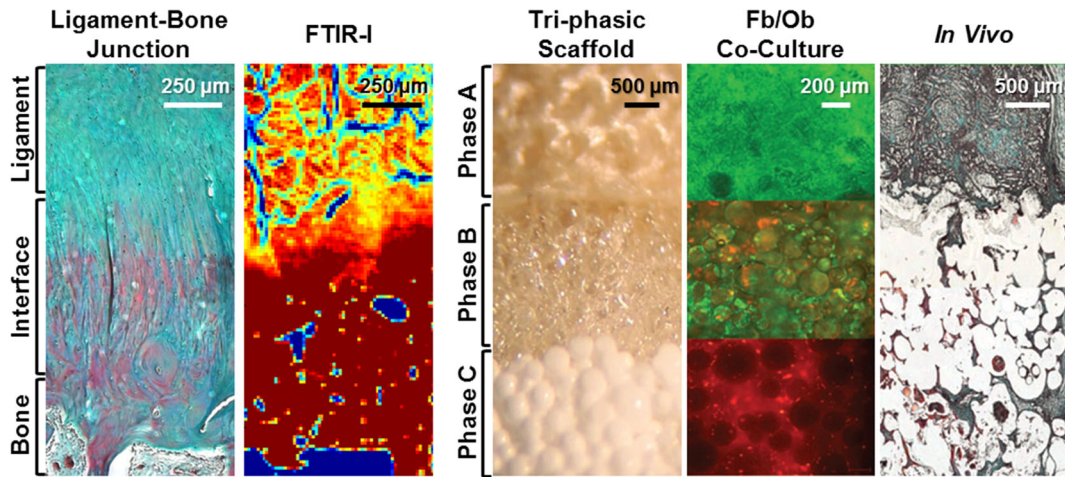
developed a continuous multi-phased synthetic ACL graft, which consisted of braided polylactide-*co*-glycolide (PLGA) microfibers arranged to form a ligament with two denser fiber regions at either end to facilitate bone formation.<sup>19,21,68</sup> *In vitro*<sup>19,68</sup> and *in vivo*<sup>21</sup> evaluation of this design in a rabbit ACL reconstruction model demonstrated biocompatibility



TABLE 1. Complex scaffold designs for integrative ligament tissue engineering.

Study	Material and scaffold design	Induction agents	Cell source	Animal model	Tissues formed*
<b>Stratified scaffold designs</b>					
Bourke <i>et al.</i> <sup>11</sup>	Poly(DTE carbonate) or PLA fibers (ligament) embedded in PMMA plugs (bone)	–	Rabbit skin fibroblasts	Rat subcutaneous implant	–
Cooper <i>et al.</i> <sup>19,21</sup> and Lu <i>et al.</i> <sup>68</sup>	Braided PGA, PLGA, or PLA fibers (ligament) with denser braided fiber ends (bone)	–	Murine BALB/C CL7 fibroblasts, <sup>19</sup> Rabbit ACL fibroblasts <sup>19,21,68</sup>	Rabbit ACL reconstruction <sup>21</sup>	Ligament
Altman <i>et al.</i> <sup>3</sup> and Horan <i>et al.</i> <sup>42</sup>	Silk yarns (ligament) connecting knitted silk ends (bone)	–	Rat BMSCs	Rat intramuscular implant, Rat subcutaneous implant, Caprine ACL reconstruction, Human ACL reconstruction	Ligament
Paxton <i>et al.</i> <sup>86,87</sup>	Fibrin gel (ligament) with PEGDA-HA hydrogel or brushite anchors (bone)	HA, brushite (bone)	Rat tendon fibroblasts, <sup>86</sup> Chick tendon fibroblasts <sup>87</sup>	–	Ligament Bone
Kimura <i>et al.</i> <sup>54</sup>	Braided PLA fibers (ligament) wrapping GF-laden gelatin hydrogel ends (bone)	bFGF (bone)	–	Rabbit ACL reconstruction	Ligament
Spalazzi <i>et al.</i> <sup>113</sup>	PLGA-BG microspheres wrapped with PLGA fiber collar (interface)	BG (OMFC)	–	Bovine patellar tendon ( <i>in vitro</i> )	Fibrocartilage
Subramony <i>et al.</i> <sup>114</sup>	Fiber collar with parallel PLGA and PLGA-HA regions (interface)	HA (MFC)	–	Rat ACL reconstruction	Fibrocartilage Bone
Lee <i>et al.</i> <sup>82</sup>	Porous PCL construct (ligament) with GF-laden heparin hydrogel ends (interface)	BMP-2 (MFC)	Rabbit ligament fibroblasts, Rabbit meniscus fibrochondrocytes	Murine subcutaneous implant	Ligament Fibrocartilage Mineralized fibrocartilage
Spalazzi <i>et al.</i> <sup>111,110</sup>	PLGA mesh (ligament) sintered to PLGA microspheres (interface), sintered to PLGA-BG microspheres (bone)	BG (bone)	Bovine ACL fibroblasts, <sup>110,111</sup> Bovine full thickness chondrocytes, <sup>110</sup> Bovine osteoblasts <sup>110,111</sup>	Rat subcutaneous implant <sup>110</sup>	Ligament Fibrocartilage Bone
Subramony <i>et al.</i> <sup>115</sup>	Braided PCL-PLGA fibers (ligament) with braided PCL-PLGA-HA fiber ends (bone), wrapped with biphasic PLGA/PLGA-HA fiber collars (interface)	HA (MFC, bone)	Rat BMSCs	Rat ACL reconstruction	Ligament Fibrocartilage Bone
Ma <i>et al.</i> <sup>71,72</sup>	Scaffold-less, MSC-derived bone-ligament-bone construct	–	Rat BMSCs, <sup>71</sup> Ovine BMSCs <sup>72</sup>	Rat MCL reconstruction, <sup>71</sup> Ovine ACL reconstruction <sup>72</sup>	Ligament
<b>Gradient scaffold designs</b>					
Samavedi <i>et al.</i> <sup>97,96</sup>	PUR fibers (ligament) with gradient to PCL-HA fibers (bone)	HA, CDA (MFC, bone)	Murine MC3T3 osteoprogenitor cells, <sup>97</sup> Rat BMSCs <sup>96</sup>	–	–
Samavedi <i>et al.</i> <sup>98</sup>	Aligned PCL fibers (ligament) with gradient to unaligned PLGA fibers (bone)	–	Rat BMSCs	–	–

\*Note Tissue formation was determined by staining, immunohistochemistry, or gene expression for pertinent matrix components (ligament: collagen I, and/or collagen III; fibrocartilage: glycosaminoglycans (GAG) and collagen; mineralized fibrocartilage: GAG, collagen, and mineral; bone: mineral and/or ALP). bFGF: basic fibroblast growth factor; BG: bioactive glass; BMP: bone morphogenetic protein; BMSCs: bone marrow-derived mesenchymal stem cells; CDA: calcium-deficient apatite; DTE: desamino tyrosyl-tyrosine ethyl ester; GF: growth factor; HA: hydroxyapatite; MFC: mineralized fibrocartilage; PCL: poly-ε-caprolactone; PEGDA: polyethylene glycol diacrylate; PGA: polyglycolide; PLA: polylactide; PLCL: polylactide-co-ε-caprolactone; PLGA: polylactide-co-glycolide; PMMA: polymethyl methacrylate; PUR: polyester urethane urea.



**FIGURE 2.** Scaffold design for *ligament-interface-bone* regeneration. Mimicking the stratified structure (Modified Goldner's Masson Trichrome)<sup>126</sup> and composition (FTIR-I: Fourier Transform infrared spectroscopy)<sup>89</sup> of the native insertion, a tri-phasic scaffold (Phase A: PLGA mesh, Phase B: PLGA microspheres, Phase C: PLGA-BG microspheres) was designed for ACL-bone interface regeneration.<sup>110,111</sup> This design allowed for spatial control over cell distribution (Fb: fibroblasts on Phase A, Ob: osteoblasts on Phase C, along with chondrocytes in a hydrogel in Phase B) enabled the formation of compositionally distinct yet structurally continuous tissue regions *in vivo* (Modified Goldner's Masson Trichrome).

and extensive collagenous tissue infiltration by 12 weeks. More recently, Altman *et al.* developed a similar multi-region silk *bone-ligament-bone* graft consisting of silk yarns connecting more densely knit regions at either end for bony attachment.<sup>3,42</sup> After 12 months of implantation in a caprine ACL reconstruction model, a collagenous ligament-like structure with aligned cells and crimped matrix was observed. To harness the potential use of growth factors to enhance graft-bone integration, Kimura *et al.* developed a multi-phased system comprised of a braided PLA-collagen scaffold with basic fibroblast growth factor-releasing gelatin hydrogels at either end to be placed within the bone tunnels.<sup>54</sup> This design supported the formation of ligament and bone regions, and resulted in enhanced tensile mechanical properties compared to single-phased controls. Similarly, Paxton *et al.* investigated the incorporation of hydroxyapatite (HA) and the RGD cell-adhesion peptide into a polyethylene glycol (PEG) hydrogel for engineering ligament-bone attachments and observed that the incorporation of HA improved interface formation.<sup>86</sup> The bioresorbable calcium phosphate brushite replaced HA in subsequent graft anchor designs,<sup>87</sup> with the two ends embedded in fibrin gel to form a *bone-ligament-bone* construct. Using a cell-based approach, Ma *et al.* formed *bone-ligament-bone* constructs through co-culture of mesenchymal stem cell (MSC)-derived bone constructs with a MSC-derived ligament monolayer rolled between.<sup>71</sup> *In vivo* evaluation in an ovine model showed graft integration with the native bone and the formation of an interface between the ligament and bone phases which structurally resembles fibrocarti-

lage.<sup>72</sup> Overall, these novel *bone-ligament-bone* designs represent significant advances in forming multi-tissue units, and, from a *strategic biomimicry* perspective, elegantly demonstrate the importance of multi-tissue over single-tissue design, especially in terms of biomimetic tissue regeneration and resultant functionality.

One of the challenges in the implementation of the *bone-ligament-bone* design is that the fibrocartilaginous interface between the ligament and bone regions is not consistently or uniformly regenerated. Structure-function studies have revealed that the ligament-bone insertion is optimized to withstand the unique combination of tensile and compressive loading sustained at this interface,<sup>7,20,75,112</sup> and is therefore critical for mediating load transfer and minimizing stress concentrations between soft tissue and bone.<sup>7,20,80</sup> As the elastic modulus of bone is more than an order of magnitude greater than that of the ligament, the gradual transition in mechanical properties facilitated by the intermediate fibrocartilage regions protects the soft tissue from contact deformation and damage at high strains.<sup>8,40</sup> Therefore, incorporating interface regeneration into graft design will be essential for achieving physiological joint function after ligament reconstruction. To this end, Spalazzi *et al.* reported on the design and optimization of a stratified *ligament-interface-bone* scaffold (Fig. 2).<sup>110,111</sup> The ligament phase was comprised of a PLGA mesh, the interface phase was comprised of sintered PLGA microspheres, and the bone phase consisted of sintered PLGA and 45S5 bioactive glass (BG) microspheres. Phases were joined together *via* solid state sintering. *In vitro* and *in vivo* tri-culture of fibroblasts, chondrocytes, and

osteoblasts on the tri-phasic scaffold led to the formation of interconnected ligament-, fibrocartilage- and bone-like matrix in each respective region (Fig. 2).<sup>110</sup> In addition to supporting multi-tissue formation, the stratified design exhibited graded mechanical properties across the scaffold, with the highest elastic modulus and yield strength in the bone phase, mimicking the mechanical transition of the native *ligament–interface–bone* junction. These studies demonstrate the utility of stratified design in engineering complex tissues as well as the importance of exercising spatial control of cell distribution in multi-tissue formation.

More recently, building upon these findings, Subramony *et al.* developed a five-phased, nanofiber-based scaffold for ACL tissue engineering.<sup>115</sup> In this design, a poly- $\epsilon$ -caprolactone (PCL)-based *bone–interface–ligament–interface–bone* scaffold was fabricated, and mechanoactive collars were applied at either ligament–bone junction to form a continuous, five-phased construct. *In vitro* evaluation of stem cell-seeded constructs showed upregulation of fibroblast, fibrochondrocyte, and osteoblast-specific markers on the ligament, interface, and bone phases, respectively. *In vivo* implantation of these scaffolds resulted in accelerated formation of mineralized tissue within the bone tunnels, as well as superior mechanical properties compared to single-phased controls. Together, these promising results emphasize that biomimetic, stratified scaffold design can allow for spatial control over the distribution of interface-relevant cell populations, facilitate formation of phase-specific matrix heterogeneity, and enable regeneration of the fibrocartilaginous transition.

Taking into consideration the mineral distribution across the calcified fibrocartilage interface,<sup>109</sup> Samavedi *et al.* employed offset co-electrospinning methods to fabricate fibrous scaffolds with a continuous gradation in polymer composition and mineral content which in turn guided osteogenic differentiation of stem cells in a gradient-dependent manner.<sup>96,97</sup> These methods have most recently been applied to form *bone–ligament–bone* scaffolds consisting of a region of aligned PCL fibers for ligament regeneration contiguous with regions of unaligned PLGA nanofibers at either end for bone regeneration.<sup>98</sup> Meanwhile, other designs have used a gradient of chemical cues, such as growth factors, to induce the formation of a graded calcified matrix. Phillips *et al.* fabricated collagen scaffolds with a compositional gradient of retroviral coating for the osteogenic transcription factor RUNX2, which induced seeded fibroblasts to produce a gradient of mineralized matrix both *in vitro* and *in vivo*.<sup>88</sup> These studies demonstrate that gradient scaffold design is a promising approach for interface

tissue engineering, with the potential to fully recapture and pre-design the micro- and nano-scale organization of the native tissue transitions. Unlike stratified scaffolds, gradient designs exhibit more gradual, continuous transitions in composition and mechanical properties. On the other hand, however, the stepwise increase in mineral content between phases of stratified scaffolds better approximates the exponential increase in mineral content across the interface regions.<sup>109</sup> Moreover, gradient scaffolds are relatively challenging to fabricate at physiologically relevant scales compared to stratified scaffolds. Therefore from a *strategic biomimicry* standpoint, it will be important to systematically investigate and compare gradient scaffolds with stratified designs and determine whether either or both are optimal for multi-tissue formation. It is also emphasized that cells and the host environment also play a role here. Namely, as the stratified or gradient-based scaffold system degrades and is remodeled by cells, a cell-engineered biomimetic gradient of composition will emerge and give rise to the physiologically relevant structure–function profile.

It is also noted that one of the challenges in stratified scaffold design is achieving functional integration of compositionally or mechanically distinct layers. While adhesives have been widely used to join scaffold or tissue phases, the addition of such materials may restrict the diffusion of nutrients, metabolites, or cytokines which are crucial for cell function and tissue development.<sup>38</sup> Moreover, a sharp transition between dissimilar materials or tissues is inherently weaker than a gradual interface consisting of interdigitated phases.<sup>63,73</sup> One strategy to circumvent this limitation is to ensure that all phases of the stratified scaffold are predominately comprised of the same type of biomaterial, such as PLGA which was used by Spalazzi *et al.* in the *ligament–interface–bone* graft.<sup>110,111</sup> Specifically, by sintering the phases beyond the glass transition temperature of PLGA, they can be joined seamlessly and functionally to prevent delamination and ensure structural continuity. More recently, Harley *et al.* demonstrated that interdigitated stratified scaffolds can be fabricated by allowing interdiffusion of liquid collagen-GAG suspensions followed by lyophilization.<sup>38</sup>

In summary, the extensive body of work on ligament–bone engineering reaffirms that integration of soft tissue to the native bone remains a primary challenge in functional ligament tissue engineering. One of the advantages of the stratified and gradient designs is that pre-engineering the ligament–bone interface *via* biomimetic scaffold designs *ex vivo*, allows for subsequent focus *in vivo* to be on the relatively easier task of facilitating bone–bone integration.



## COMPLEX SCAFFOLD DESIGN FOR INTEGRATIVE TENDON TISSUE ENGINEERING

Similar to the ligament, the functional tendon, which joins muscle to bone, is a multi-tissue structure consisting of structurally contiguous yet compositionally distinct regions: *muscle–interface–tendon–interface–bone*. Like the ACL, major tendons, such as those of the rotator cuff, insert into subchondral bone through a graded fibrocartilage transition, divided into non-mineralized and mineralized regions.<sup>7,10,20</sup> A number of studies have shown that the region between tendon and bone is relatively compliant, with a tensile modulus that is approximately half that of the tendon,<sup>43,99,121</sup> which minimizes the formation of stress concentrations at the interface.<sup>66</sup> As the tendon–bone and ligament–bone interfaces are similar in structure, function, and composition, many of the multi-phasic and gradient scaffold design strategies discussed above, as well as criteria for mechanical and compositional evaluation, can also be applied for functional and integrative tendon tissue engineering. The ideal tendon scaffold should similarly incorporate structural and compositional heterogeneity which enable well-defined, phase-specific changes in mechanical properties and support interactions amongst heterotypic cell populations. Currently, in addition to the tendon proper, many studies have focused on engineering either the *tendon–interface–bone* (Table 2) or *muscle–interface–tendon* (Table 3) unit. It is noted that despite similarities between tendon and ligament, the scaffold design must also be adapted to account for the tendon-specific loading environment. While both of these connective tissues withstand high tensile loads, tendons typically experience loading in a uniaxial direction, in contrast to ligaments which are also loaded in torsion.<sup>94</sup> Furthermore, current surgical repair methods unique to the anatomic location and disease condition of the joint must also be considered.

Rotator cuff tears represent one of the most common tendon injuries that necessitate clinical intervention. However, unlike treatment strategies for ligament injuries, which are dominated by reconstructions, tendon injuries are managed clinically *via* repair whereby the tendon is reattached to bone by mechanical means. However, restoration of the native tendon–bone insertion is challenging and tendon detachment remains the primary cause of surgical failure. To improve fixation, Chang *et al.* and Sundar *et al.* have shown that surgically interposing periosteum tissue<sup>14</sup> or demineralized bone matrix<sup>116</sup> between the native tendon and bone helps to facilitate the development of a fibrocartilage-like matrix and improve mechanical function. However, the clinical relevance of such methods is limited by the challenges associated with

harvesting and preparing these additional tissues during repair procedures. Focusing on the fibrocartilaginous tendon–bone interface and taking into consideration current cuff repair surgical techniques, Moffat *et al.* designed a biphasic scaffold consisting of contiguous layers of aligned PLGA and PLGA-HA nanofibers joined *via* electrospinning, intended to mimic the non-calcified and calcified fibrocartilage regions, respectively (Fig. 3).<sup>78</sup> *In vivo* evaluation in both rodent<sup>78</sup> and ovine<sup>134</sup> rotator cuff repair models using this scaffold as an inlay between tendon and bone resulted in the formation of a fibrocartilage-like matrix in both scaffold phases (Fig. 3). Mineral distribution was maintained, in which calcified fibrocartilage formed only on the HA-containing phase. Pre-seeding the biphasic scaffold with bone marrow-derived cells also promoted fibrocartilage matrix maturation and enhanced collagen organization at the tendon–bone junction. From a biomimetic scaffold design perspective, it was found that regeneration of an organized interface was only evident with the biphasic design, but not when the tendon was repaired with either single-phased PLGA or PLGA-HA only scaffolds (Fig. 3). These observations suggest that the mineral-free top layer of the biphasic scaffold guides tendon and fibrocartilage formation, with nanofiber alignment promoting integration with tendon, while the controlled spatial distribution of mineral content in the bottom layer of the scaffold supports calcified fibrocartilage formation and osteointegration.

A number of gradient scaffold designs have also been explored for tendon–bone integration, seeking to pre-engineer the mineral gradient<sup>34</sup> at the tendon–bone junction by employing various methods of calcium phosphate incorporation. For example, Li *et al.* developed a simple and elegant coating method to generate a linear gradient of calcium phosphate on polymeric nanofiber scaffolds by varying the incubation time of these scaffolds in a concentrated simulated body fluid.<sup>64</sup> It was reported that the mineral distribution imparted a gradation in mechanical properties along the length of the scaffold. The system was then further optimized by increasing the concentration of bicarbonate ions in the soaking solution, which resulted in denser mineral coating on the fibers and further improved mechanical properties.<sup>67</sup> This graded scaffold was shown to exhibit spatial control over osteogenesis of adipose-derived MSCs, with more extensive staining of osteogenic markers observed on areas of higher scaffold mineral content.<sup>65</sup> Another novel gradient scaffold design focused on protein distribution, whereby a fibronectin concentration gradient was generated on polymer nanofiber scaffolds and was shown to exhibit control over density and morphology of cultured fibroblasts.<sup>105</sup> Also using con-

TABLE 2. Complex scaffold designs for integrative tendon tissue engineering (tendon-bone).

Study	Material and scaffold design	Induction agents	Cell source	Animal model	Tissues formed*
<b>Stratified scaffold designs</b>					
Dickerson <i>et al.</i> <sup>24</sup>	Demineralized bone construct (tendon) with non-demineralized bone end	–	–	Ovine rotator cuff repair	Fibrocartilage Mineralized fibrocartilage Bone
Moffat <i>et al.</i> <sup>79,78</sup> and Zhang <i>et al.</i> <sup>134</sup>	Patch with parallel PLGA and PLGA-HA fiber regions (inter-face)	HA (MFC)	Bovine tendon fibroblasts, Bovine full thickness chondrocytes	Rat subcutaneous implant, <sup>78</sup> Rat rotator cuff repair, <sup>78,88</sup> Ovine rotator cuff repair <sup>88</sup>	Fibrocartilage Mineralized fibrocartilage
<b>Gradient scaffold designs</b>					
Phillips <i>et al.</i> <sup>86</sup>	Fibrous collagen constructs (soft tissue) with graded RUNX-2 retrovirus coating (bone)	RUNX-2 retrovirus (MFC, bone)	Rat skin fibroblasts	Rat subcutaneous implant	Bone
Eriskien <i>et al.</i> <sup>29</sup>	PCL fibers (soft tissue) with gradient to PCL-TCP fibers (bone)	TCP (MFC, bone)	Murine MC3T3 osteoprogenitor cells	–	Bone
Cui <i>et al.</i> <sup>22,23</sup> and Zou <i>et al.</i> <sup>139</sup>	PLA fibers (tendon) with graded HA coating (bone)	HA (MFC, bone)	Murine MC3T3 osteoprogenitor cells	–	–
Li <i>et al.</i> <sup>64</sup> and Liu <i>et al.</i> <sup>67,65</sup>	PLGA fibers (tendon) with graded HA coating (bone)	HA (MFC, bone)	Murine MC3T3 osteoprogenitor cells, <sup>64</sup> Rat ADSCs <sup>65</sup>	–	Bone

\*Note Tissue formation was determined by staining, immunohistochemistry, or gene expression for pertinent matrix components (tendon: collagen, collagen I, and/or collagen III; fibrocartilage: glycosaminoglycans (GAG) and collagen; mineralized fibrocartilage: GAG, collagen, and mineral; bone: mineral and/or ALP). ADSCs: adipose-derived mesenchymal stem cells; HA: hydroxyapatite; MFC: mineralized fibrocartilage; PCL: poly- $\epsilon$ -caprolactone; PLA: polylactide; PLGA: polylactide-co-glycolide; RUNX-2: runt-related transcription factor; TCP:  $\beta$ -tricalcium phosphate.



**TABLE 3. Complex scaffold designs for integrative tendon tissue engineering (muscle–tendon).**

Study	Material and scaffold design	Induction agents	Cell source	Animal model	Tissues formed*
Swasdison <i>et al.</i> <sup>117,118</sup>	Collagen I gel ( <i>muscle</i> )	–	Quail pectoral myoblasts, <sup>117</sup> Chick tendon fibroblasts <sup>118</sup>	–	Muscle Tendon
Ladd <i>et al.</i> <sup>58</sup>	PCL-collagen I fibers ( <i>muscle</i> ) with gradient to PLA-collagen I fibers ( <i>tendon</i> )	–	Murine C2C12 myoblasts, Murine NIH3T3 fibroblasts	–	–
Larkin <i>et al.</i> <sup>60</sup> and Kostrominova <i>et al.</i> <sup>57</sup>	Scaffold-less, cell-based <i>muscle–tendon</i> construct	–	Rat soleus myocytes, Rat tendon fibroblasts	–	Muscle Interface Tendon

\*Note Tissue formation was determined by staining, immunohistochemistry, or gene expression for pertinent matrix components (muscle: myosin; interface: paxillin; tendon: collagen, collagen I, and/or collagen III). PCL: poly-ε-caprolactone; PLA: polylactide.

trolled soaking methods, Dickerson *et al.* recently developed a regionally demineralized bone-based scaffold for tendon-bone integration.<sup>24</sup> Evaluation of the scaffold in an ovine rotator cuff repair model showed that the scaffold also facilitated formation of fibrocartilaginous tissue at the tendon-bone junction, albeit the neo-fibrocartilage was thicker than that of the native insertion. An alternative method for controlling nucleation and growth of HA crystals on nanofibers was reported by Cui *et al.*, whereby PLA fibers were functionalized with carboxyl, hydroxyl, and amino groups, which served as induction sites for *in situ* HA formation.<sup>22,23</sup> This method was applied to fabricate fibrous scaffolds with graded HA content which supported spatial control over MC3T3 cell density, osteogenesis, and collagen deposition.<sup>139</sup> These studies demonstrate the potential of gradient-based scaffolds for composite tissue formation. The next frontier in the design of these novel scaffolds is to achieve physiologically relevant gradient profiles with micro- and nano-scale compositional changes across the scaffold length.

While the majority of tendon injuries occur in either the tendon proper or the tendon-bone insertion, muscle atrophy and detachment from tendon have also been associated with tendon degeneration. The native muscle–tendon junction serves to distribute mechanical loads between skeletal muscle and bone<sup>132</sup> and consequently the reestablishment of this interface is also important for full restoration of musculoskeletal function following injury. Paralleling the previously discussed tissue interfaces, the muscle–tendon interface represents a junction between tissues with vastly different mechanical properties. In particular, the tendon is significantly stiffer than muscle, with reported elastic modulus values as high as three orders of magnitude greater than those of muscle.<sup>83,131</sup> The native interface

between muscle and tendon consists of an interdigitating band of fibroblast-laden tissue which connects elastic muscle fibers to dense tendon collagen fibers (Fig. 1).<sup>123</sup> This inter-digitation results in an approximate ten-fold increase in muscle–tendon contact surface area and serves to distribute stresses induced by muscle contraction over a wide area, thereby minimizing the risk of tearing.<sup>122–124</sup> Thus, an ideal scaffold for muscle–tendon interface repair should also be multi-phasic in design, mimicking the different mechanical profiles of the adjacent muscle and tendon regions. Structurally and compositionally, muscle and tendon are also distinct, and engineered muscle should be distinguishable from tendon by the presence of multi-nucleated myotubes.

Early efforts to engineer the muscle–tendon interface involved culturing myoblasts in collagen gels *in vitro*, which resulted in the formation of contractile muscle constructs with fibril terminals similar to those found at the native junction.<sup>117,118</sup> Using a cell-based approach, Larkin *et al.* co-cultured skeletal muscle and engineered tendon constructs *in vitro* to form a *muscle–interface–tendon* construct.<sup>60</sup> The neo-interface region exhibited upregulated expression of muscle–tendon junction-specific paxillin, and was able to sustain tensile loading at super-physiologic strain rates. Furthermore, microscopic evaluation of the constructs revealed the termination sites of the engineered myofibers also resembled the structures found at the fetal muscle–tendon junction.<sup>57</sup> More recently, Ladd *et al.* developed a tri-phasic scaffold for engineering a *muscle–interface–tendon* unit by co-electrospinning PCL-collagen and PLA-collagen onto opposite ends of a single mandrel.<sup>58</sup> The resulting scaffolds exhibited a similar spatial strain distribution as the native muscle–tendon interface and facilitated both myoblast and fibroblast attachment.

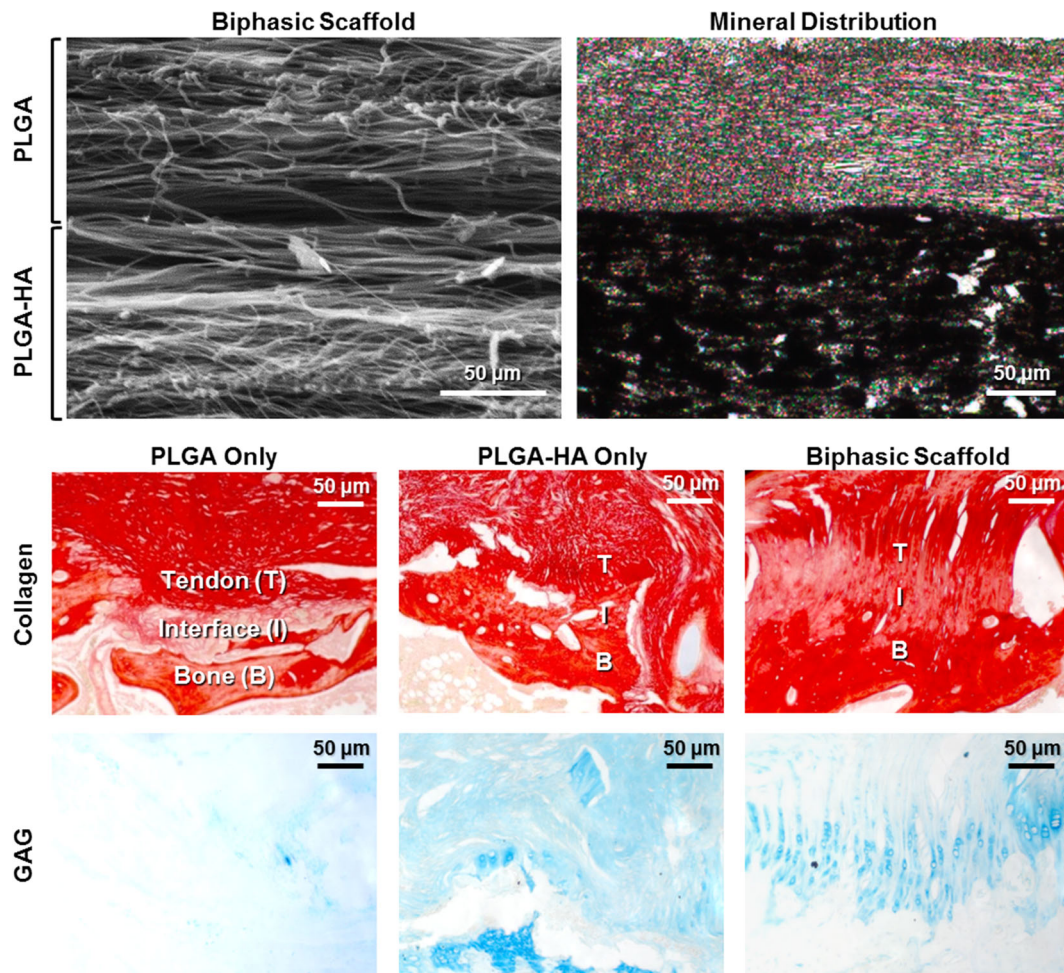


**FIGURE 3.** Scaffold design for *tendon-interface-bone* regeneration.<sup>78</sup> A biphasic scaffold comprised of layered aligned PLGA and PLGA-HA nanofibers was fabricated by electrospinning, which led to phase-specific mineral deposition *in vivo* (Von Kossa, subcutaneous athymic rat model). The bilayer scaffold was subsequently tested in a rat rotator cuff repair model, and disorganized scar tissue was observed in the single-phased controls (PLGA, PLGA-HA only). Interestingly, tendon-bone integration *via* an organized bilayer fibrocartilage interface was only observed with the biphasic design (Picrosirius red, Alcian blue).

In summary, current scaffold design approaches in integrative tendon repair are a reflection of the prevalence of tendon injuries and current clinical practice, and complex scaffold designs in the form of stratified or gradient design are promising approaches for functional and integrative tendon tissue engineering.

### COMPLEX SCAFFOLD DESIGN FOR INTEGRATIVE CARTILAGE TISSUE ENGINEERING

Similar to the other soft connective tissues discussed here, articular cartilage health and function is intimately tied to the subchondral bone.<sup>138</sup> Structurally, the two tissue types are connected *via* the osteochondral interface, which consists of a calcified cartilage barrier that is instrumental for load bearing and force

distribution across these tissues.<sup>12,91,108</sup> Specifically, the mineral is localized to the calcified cartilage and bone regions (Fig. 4), with an exponential increase in mineral content between non-calcified and calcified regions that persists with age.<sup>51</sup> The modulus of the calcified cartilage layer is intermediate between that of articular cartilage and bone,<sup>76</sup> resulting in a gradation in mechanical properties which enables force transmission across the system while reducing the formation of stress concentrations at the soft tissue-bone interface.<sup>84,85</sup> Thus, in addition to meeting the complex mechanical demands of articulation, the ideal cartilage scaffold must also enable cartilage-bone integration by connecting these two tissues through a stable and physiologically relevant calcified cartilage layer. In other words, consideration of multi-tissue regeneration (i.e., *cartilage-bone*, *cartilage-interface*, *cartilage-interface-bone*) is also functionally relevant for inte-

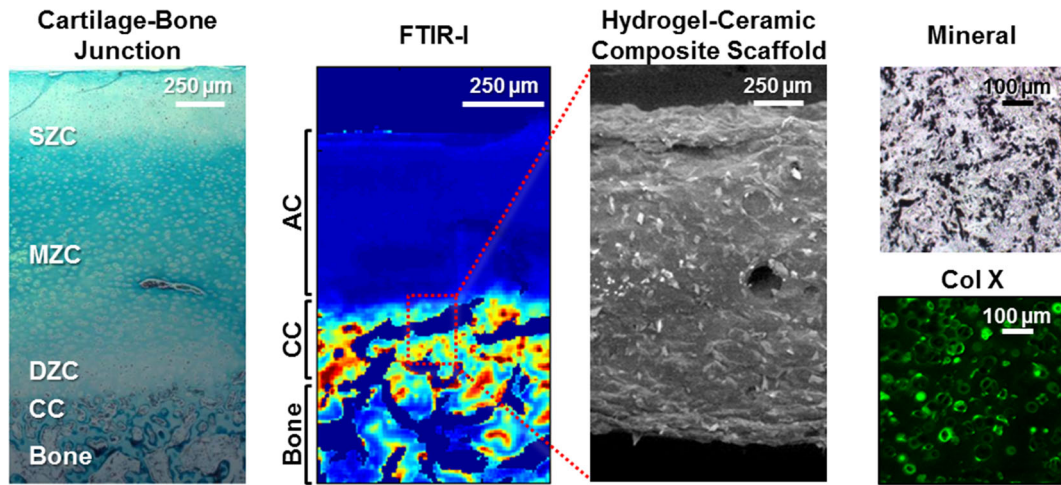


**FIGURE 4.** Hydrogel-ceramic composite scaffold for osteochondral interface regeneration. Articular cartilage (AC) connects to subchondral bone via the osteochondral interface, which consists of calcified cartilage (CC, Modified Goldner's Masson Trichrome). Analysis via Fourier Transform infrared spectroscopy (FTIR-I) reveals an exponential increase in mineral content between the articular cartilage and calcified cartilage regions.<sup>51</sup> The hydrogel-HA composite design<sup>52</sup> guided chondrocyte-mediated deposition of a mineralized matrix (Von Kossa) that is positive for collagen X (immunohistochemistry) and can be used in conjunction with cartilage grafts.

grative cartilage repair (Table 4). The mechanical functionality of regenerated tissue should therefore be evaluated by compressive mechanical testing while matrix composition should be evaluated by histology and immunohistochemistry. Cartilage tissue is comprised of a GAG and collagen II-rich matrix while calcified cartilage is characterized by the additional presence of collagen X and mineral.

A number of stratified cartilage–bone designs have been developed and evaluated for osteochondral tissue engineering. As they have been thoroughly reviewed elsewhere,<sup>46,61,120</sup> only a brief summary is provided below. Early designs consisted predominantly of fusing distinct cartilage and bone regions together through the use of sutures or glue. For example, Schaefer *et al.* developed a biphasic scaffold by suturing chondrocyte-seeded PLGA meshes with periosteal cell-seeded PLGA/PEG foams.<sup>100</sup> Early cell–cell interactions proved vital to osteochondral interface formation, as integration was enhanced when the constructs were sutured together 1 week post-seeding as opposed to 4 weeks.<sup>100</sup> Later, Gao *et al.* joined a stem cell-seeded hyaluronan sponge with a porous stem cell-seeded calcium phosphate scaffold using fibrin glue and reported the formation of continuous collagen fibers between the two phases in a subcutaneous rat model.<sup>33</sup> Similarly, Alhadlaq and Mao developed a bi-layered, PEG-based hydrogel osteochondral construct by sequential photo-polymerization, where the top and bottom hydrogel layers contained stem cell-derived chondrocytes and osteoblasts, respectively.<sup>1</sup> Distinct but histologically integrated cartilaginous and osseous

regions developed after subcutaneous implantation in athymic mice, albeit it is unclear whether consistent or uniform osteochondral interface formation was achieved. Comparable results were obtained from other stem cell-seeded biphasic scaffold designs.<sup>16,32,37,47,103,119</sup> Collectively, these studies demonstrate the feasibility of engineering both cartilage- and bone-like tissues. However, similar to other soft tissue–bone designs discussed above, these biphasic scaffolds are for engineering cartilage and bone, while the osteochondral interface between the two tissues has been underemphasized in these designs. The significance of the interface as a structural barrier protecting the healing cartilage from vascular invasion was demonstrated by Hunziker *et al.* using a full-thickness cartilage defect model and a Gore-Tex<sup>®</sup> membrane with a 0.2 µm pore diameter.<sup>45</sup> Placing the membrane between cartilage and bone compartments preserved the integrity of newly formed cartilage, limiting vascular ingrowth from the subchondral bed, and preventing ectopic mineralization. Taking the osteochondral interface into consideration, Aydin *et al.* designed a biphasic scaffold whereby a PLA-PCL bone region with vertical channels was combined with a PGA cartilage region using a pigmented polymeric blend that allowed for visualization of the interface region. Scanning electron microscopy and micro-CT imaging showed the establishment of cartilage- and bone-like regions, as well as an interface region, although biochemical composition of the regenerated tissues was not determined. To more closely mimic the native osteochondral junction, Jiang *et al.* developed



TABLE 4. Complex scaffold designs for integrative cartilage tissue engineering.

Study	Material and scaffold design	Induction agents	Cell source	Animal model	Tissues formed*
<b>Stratified scaffold designs</b>					
Schaefer <i>et al.</i> <sup>100</sup>	PGA mesh ( <i>cartilage</i> ) sutured to PLGA-PEG foam ( <i>bone</i> )	–	Bovine full thickness articular chondrocytes, Bovine ulnar diaphysis periosteal cells	–	Cartilage Bone
Scotti <i>et al.</i> <sup>101</sup>	Collagen I and III matrix ( <i>cartilage</i> ) joined to devitalized <i>bone</i> with fibrin	–	Human full thickness articular chondrocytes	–	Cartilage Bone
Ibrahim <i>et al.</i> <sup>47</sup>	Layered PVA-NOCC ( <i>cartilage</i> ) and PVA-NOCC-HA ( <i>bone</i> ) gels	–	Human BMSCs	Rat subcutaneous implant	Cartilage Bone
Alhadlaq and Mao <sup>1</sup>	Layered PEGDA gel <i>cartilage–bone</i> constructs	Pre-differentiation with TGF- $\beta$ 1 ( <i>cartilage</i> ) or DEX/ $\beta$ -GP/AA ( <i>bone</i> )	Rat BMSCs	Murine subcutaneous implant	Cartilage Calcified cartilage Bone
Grayson <i>et al.</i> <sup>37</sup>	Agarose hydrogel ( <i>cartilage</i> ) and decellularized <i>bone</i> cores ( <i>bone</i> )	Pre-differentiation with TGF- $\beta$ 3 ( <i>cartilage</i> ) or DEX/ $\beta$ -GP/AA ( <i>bone</i> )	Human BMSCs	–	Cartilage Bone
Galperin <i>et al.</i> <sup>32</sup>	Poly(HEMA) hydrogel ( <i>cartilage</i> ) coated with HA ( <i>bone</i> )	Pre-differentiation with TGF- $\beta$ 1 ( <i>cartilage</i> )	Human BMSCs	–	Cartilage Bone
Chen <i>et al.</i> <sup>15</sup>	Plasmid GF-activated chitosan–gelatin ( <i>cartilage</i> ) and plasmid GF-activated chitosan–gelatin–HA ( <i>bone</i> ) hydrogels	Plasmid TGF- $\beta$ 1 ( <i>cartilage</i> )	Rabbit BMSCs	Rabbit osteochondral defect	Cartilage Bone
Re'em <i>et al.</i> <sup>92</sup>	Layered GF/affinity-bound alginate hydrogel <i>cartilage–bone</i> constructs	BMP-2 ( <i>bone</i> )	Human BMSCs	Rabbit osteochondral defect	Cartilage Bone
Seo <i>et al.</i> <sup>131</sup>	Layered GF-laden gelatin–TCP sponge <i>cartilage–bone</i> constructs	TGF- $\beta$ 1 ( <i>cartilage</i> ), BMP-4 ( <i>bone</i> )	Equine BMSCs	Equine osteochondral defect	Cartilage Bone
Castro <i>et al.</i> <sup>13</sup>	PEG-PEGDA hydrogel with GF-encapsulated PLGA nanospheres ( <i>cartilage</i> ) and PCL-PEGDA-HA composite with GF-encapsulated PDO nanospheres ( <i>bone</i> )	PRP ( <i>cartilage</i> ), BMP-2 ( <i>bone</i> )	Human BMSCs	–	Cartilage Bone
Chiang <i>et al.</i> <sup>18</sup>	Porous PLGA plug ( <i>cartilage</i> ) fit into a PLGA-TCP chamber ( <i>bone</i> )	TCP ( <i>bone</i> )	Human full thickness chondrocytes	Human osteochondral lesion	–
Ding <i>et al.</i> <sup>25</sup>	Fibrous PGA-PLA ( <i>cartilage</i> ) and PCL-HA ( <i>bone</i> ) constructs	HA ( <i>bone</i> )	Caprine full thickness chondrocytes, Caprine BMSCs	Murine subcutaneous implant	Cartilage Bone
Yunos <i>et al.</i> <sup>133</sup>	PLA fibers ( <i>cartilage</i> ) coating a BG-polyurethane foam ( <i>bone</i> )	BG ( <i>bone</i> )	Murine ATDC5 chondrocytes	–	–
Zhang <i>et al.</i> <sup>135</sup>	Porous collagen I construct ( <i>cartilage</i> ) integrated with PLA fibers ( <i>bone</i> )	–	Rabbit BMSCs	Rabbit osteochondral defect	Cartilage Bone
Bernstein <i>et al.</i> <sup>9</sup>	Cell layer ( <i>cartilage</i> ) on top of porous TCP ( <i>bone</i> )	TCP ( <i>bone</i> )	Ovine full thickness patellar chondrocytes	Ovine osteochondral defect	Cartilage Bone
Khanarian <i>et al.</i> <sup>53</sup>	Stratified alginate–HA composite hydrogel ( <i>interface</i> )	HA (CC)	Bovine articular deep zone chondrocytes	–	Calcified cartilage
Khanarian <i>et al.</i> <sup>52</sup>	Stratified agarose–HA composite hydrogel ( <i>interface</i> )	HA (CC)	Bovine articular deep zone chondrocytes	–	Calcified cartilage

TABLE 4. continued.

Study	Material and scaffold design	Induction agents	Cell source	Animal model	Tissues formed*
Heymer <i>et al.</i> <sup>41</sup>	Collagen I matrix with hyaluronan gel (cartilage), PLA (interface), and porous PLA-HA-TCP construct (bone)	HA, TCP (bone)	Human BMSCs	–	Cartilage
Lu <i>et al.</i> <sup>69</sup> and Jiang <i>et al.</i> <sup>49</sup>	Agarose hydrogel (cartilage), agarose with PLGA-BG microspheres (interface), and PLGA-BG microspheres (bone)	BG (CC, bone)	Human osteosarcoma cells, <sup>69</sup> Human osteoblast-like cells, <sup>69</sup> Bovine articular full thickness chondrocytes, <sup>49</sup> Bovine osteoblasts <sup>49</sup>	–	Cartilage Calcified cartilage Bone
Kon <i>et al.</i> <sup>56,55</sup>	Fibrous collagen I (cartilage), 60:40 collagen I:HA (interface), and 30:70 collagen I:HA (bone) constructs	HA (CC, bone)	–	Equine osteochondral defect, <sup>56</sup> Human osteochondral lesion <sup>55</sup>	Cartilage Bone
Marquass <i>et al.</i> <sup>74</sup>	Collagen I hydrogel (cartilage), activated plasma (interface), and TCP matrix (bone)	TCP (bone)	Ovine BMSCs	Ovine osteochondral defect	Cartilage Bone
Cheng <i>et al.</i> <sup>17</sup>	Collagen I microspheres with differentiated MSCs (cartilage and bone) joined by a collagen gel with undifferentiated MSCs (interface)	Pre-differentiation with TGF- $\beta$ 1 (cartilage) or DEX/ $\beta$ -GP/AA (bone)	Rabbit BMSCs	–	Cartilage Calcified cartilage Bone
Aydin <i>et al.</i> <sup>6</sup>	PGA nonwoven felt layer (cartilage) connected to a collagen I and HA-coated PLLA-PCL sponge (bone) via a PLLA-PCL layer (interface)	HA (bone)	Murine L929 fibroblasts	–	–
Gradient scaffold designs Zhang <i>et al.</i> <sup>137</sup>	Polysulfone or cellulose acetate and BG cartilage–bone constructs with gradient in porosity	BG, HCA (CC, bone)	–	–	–
Salerno <i>et al.</i> <sup>95</sup>	PCL foam cartilage–bone construct with gradients in pore size, porosity, and HA	HA (CC, bone)	–	–	–
Aviv-Gavriel <i>et al.</i> <sup>5</sup>	Gelatin hydrogel cartilage–bone constructs with CaP gradient	CaP(CC, bone)	–	–	–
Sherwood <i>et al.</i> <sup>104</sup>	Porous PLGA-PLA construct (cartilage) with gradient to PLGA-TCP construct (bone)	TCP (CC, bone)	Ovine full thickness articular chondrocytes	–	Cartilage
Harley <i>et al.</i> <sup>39</sup> and Getgood <i>et al.</i> <sup>36</sup>	Porous collagen II-GAG construct (cartilage) with gradient to collagen I-GAG-CaP (bone)	CaP(CC, bone)	–	Caprine osteochondral defect <sup>36</sup>	Cartilage
Eriskien <i>et al.</i> <sup>30</sup>	PCL-insulin fibers (cartilage) with gradient to PCL- $\beta$ -GP fibers	Insulin (cartilage), $\beta$ -GP (CC, bone)	Human ADSCs	–	Cartilage Bone
Singh <i>et al.</i> <sup>106</sup>	PLGA microspheres (cartilage) with gradient to PLGA-CaCO <sub>3</sub> or PLGA-TiO <sub>2</sub> microspheres (bone)	CaCO <sub>3</sub> , TiO <sub>2</sub> (CC, bone)	Human UCMSCs	–	–

TABLE 4. continued.

Study	Material and scaffold design	Induction agents	Cell source	Animal model	Tissues formed*
Wang <i>et al.</i> <sup>128</sup>	Alginate and PLGA microsphere or porous silk and silk microsphere cartilage–bone constructs with opposing GF gradients	IGF-1 (cartilage), BMP-2 (bone)	Human BMSCs	–	Cartilage Bone
Dormer <i>et al.</i> <sup>26,27</sup>	PLGA microsphere cartilage–bone constructs with opposing GF gradients	TGF- $\beta$ 1 (cartilage), BMP-2 (bone)	Human BMSCs <sup>26</sup> UCMSCs <sup>26,27</sup>	Rabbit osteochondral defect <sup>27</sup>	Cartilage Bone
Mohan <i>et al.</i> <sup>81,82</sup>	PLGA microsphere cartilage–bone constructs with opposing GF and/or EOM material gradients	TGF- $\beta$ 1 <sup>81</sup> or TGF- $\beta$ 3 <sup>82</sup> and/or CS <sup>82</sup> (cartilage), BMP-2 <sup>81,82</sup> and/or BG <sup>82</sup> and/or HA <sup>81</sup> (bone)	Rat BMSCs <sup>82</sup>	Rabbit osteochondral defect	Cartilage Bone

\*Note Tissue formation was determined by staining, immunohistochemistry, or gene expression for pertinent matrix components (cartilage: GAG and collagen II; calcified cartilage: collagen X or glycosaminoglycan (GAG) and mineral; bone: mineral, calcium deposition, collagen I, bone sialoprotein and/or ALP). AA: ascorbic acid; ADSCs: adipose-derived mesenchymal stem cells; BG: bioactive glass;  $\beta$ -GP:  $\beta$ -glycerolphosphate; BMP: bone morphogenetic protein; BMSCs: bone marrow-derived mesenchymal stem cells; CaP: calcium phosphate; CC: calcified cartilage; CS: chondroitin sulfate; DEX: dexamethasone; GF: growth factor; HA: hydroxyapatite; HCA: hydroxycarbonate apatite; HEMA: hydroxyethyl methacrylate; IGF: insulin-like growth factor; PCL: poly- $\epsilon$ -caprolactone; PDO: polydioxanone; PEG: polyethylene glycol; PEGDA: PEG diacrylate; PGA: polylactide; PLA: polylactide; PLGA: polylactide-co-glycolide; PRP: platelet rich plasma; PVA-NOCC: polyvinyl alcohol-N,O-carboxymethylated chitosan; TCP:  $\beta$ -tricalcium phosphate; TGF: transforming growth factor; UCMSCs: umbilical cord mesenchymal stem cells.

a stratified *cartilage–interface–bone* scaffold consisting of a hydrogel-based region for cartilage regeneration, a hybrid hydrogel and polymer-ceramic composite microsphere region for interface regeneration, and a polymer-ceramic composite microsphere region for bone regeneration.<sup>49,69</sup> Chondrocyte and osteoblast co-culture on this scaffold system resulted in the formation of distinct yet continuous cartilaginous and osseous matrices, as well as a calcified interfacial region largely due to the pre-engineered mineralized scaffold phase.

Cell-based approaches for cartilage–bone integration were pioneered by Kandel *et al.*, and have laid the foundation for current approaches to osteochondral interface regeneration. For example, Kandel *et al.* seeded deep zone chondrocytes (DZC) on collagen II pre-coated filter inserts and observed the formation of mineralizing matrix in the region directly adjacent to the inserts.<sup>50</sup> In a follow-on study, Allan *et al.* seeded DZCs at high density on porous calcium polyphosphate scaffolds in media containing  $\beta$ -glycerophosphate ( $\beta$ -GP). A semi-crystalline calcium phosphate-containing matrix formed adjacent to the scaffold, suggesting that DZCs are a promising cell population for calcified cartilage formation.<sup>2</sup> Building on this work and focusing specifically on the osteochondral interface, Khanarian *et al.* evaluated both degradable (alginate)<sup>53</sup> and non-degradable (agarose)<sup>52</sup> hydrogel–mineral composite scaffolds for calcified cartilage formation (Fig. 4). Both scaffold systems were found to promote the deposition of a collagen II and proteoglycan-rich matrix by DZCs, resulting in enhanced compressive and shear mechanical properties, as well as chondrocyte hypertrophy and collagen X deposition (Fig. 4). Most importantly, the scaffolds supported calcified cartilage formation. The advantage of the scaffold-based approach is that fewer cells are required to achieve superior functional mechanical properties. Moreover, scaffolds can be modified prior to implantation to further enhance mechanical performance and, clinically, they may be used in conjunction with a cartilage graft for repairing full-thickness defects.

Given the mineral transition which inherently occurs across the osteochondral interface, gradient scaffolds have also been investigated for integrative cartilage repair. As heterogeneous mechanical and chemical properties must be established and maintained across the cartilage–bone interface, compositional and/or chemical gradients can also allow for regional control of cell and tissue phenotypes. Sherwood *et al.* established one of the earliest gradient osteochondral scaffold designs by using 3D printing technology to fabricate an osteochondral graft with graded variation in porosity and ceramic composition.<sup>104</sup> Chondrocytes were found to preferentially



attach to the cartilaginous phase and the tensile strength of the bone region was comparable to that of native tissue. More recently, Singh *et al.* developed a PLGA microsphere scaffold which exhibited continuous gradients in compressive mechanical properties, achieved by encapsulating a higher stiffness nanophasic material into portions of the microspheres.<sup>106</sup> Another interesting system developed by Aviv-Gavriel *et al.* consists of a gelatin membrane with a ceramic gradient formed by exposing one side of the calcium or phosphate ion-containing gels to a solution of the complementary ion.<sup>5</sup> This resulted in the formation of a partially calcified hydrogel membrane which can be adapted for integration of cartilage grafts with bone. Combining elements of both stratified and gradient designs, Harley *et al.* fabricated layered collagen-GAG scaffolds consisting of distinct cartilage and bone regions connected by a continuous interface *via* liquid-phase co-synthesis.<sup>39</sup> This unique method of fabrication resulted in small gradients of dissimilar materials extending across a soft interface. *In vivo* evaluation of the acellular scaffold in a caprine model revealed that this design supported significant formation of both cartilaginous and osseous tissue on the respective phases.<sup>36</sup> Using a novel electrospinning method, Erisken *et al.* fabricated PCL nanofiber scaffolds containing a linear tricalcium phosphate (TCP) gradient,<sup>29</sup> and the graded calcified matrix was maintained by cultured MC3T3 cells. It is emphasized that in this study, the scaffold exhibited a compositional gradient that is relevant at the physiological scale (~100  $\mu\text{m}$ ).

In order to engineer a growth factor gradient, Wang *et al.* developed a silk-based microsphere scaffold system capable of generating opposing insulin-like growth factor-1 and bone morphogenetic protein (BMP)-2 gradients *via* spatially- and temporally-controlled delivery.<sup>128</sup> Human MSCs seeded on the scaffold underwent chondrogenic and osteogenic differentiation along the growth factor concentration gradients. Similarly, Dormer *et al.* generated opposing, spatially defined mixtures of transforming growth factor- $\beta$ 1 and BMP-2 on a PLGA microsphere-based scaffold, which led to the formation of both cartilage-like and bone-like matrix in a rabbit mandibular condyle defect model.<sup>26</sup> While scaffolds with dual growth factor gradients did not out-perform sham defects in the mandibular model,<sup>27</sup> bone regeneration was enhanced in a rabbit knee model when both growth factor and HA gradients were simultaneously incorporated into the scaffold design.<sup>81</sup> These studies and others<sup>82</sup> collectively demonstrate the promise of coupling growth factor and compositional gradients for enhancing composite tissue formation, and the impact of non-growth factor inductive agents (e.g., HA) for directing tissue regeneration.

In summary, composite scaffold designs in both stratified and gradient form can be used to engineer *cartilage-interface* or *cartilage-interface-bone* grafts. The success of these tissue regeneration approaches will depend on defect site and animal model used for evaluation, and both compositional and growth factor gradients may be required for functional multi-tissue formation.

## SUMMARY AND FUTURE DIRECTIONS

An overview of current concepts in engineering complex tissues for musculoskeletal soft tissue repair, with an emphasis on scaffold design strategies that enable physiologic tissue connectivity and multi-tissue regeneration has been presented here. These biomimetic scaffold designs seek to recapitulate the spatial distribution in compositional, structural, and mechanical properties inherent between bone and soft tissues, especially across the native tissue-tissue junctions. These studies have collectively delineated several *strategic biomimicry* design principles for multi-tissue regeneration. First, one-tissue centric, single-phased scaffold systems are insufficient for recapitulating soft tissue functionality, especially when it comes to achieving graft integration with host tissues. Next, incorporation of physiologically relevant interface regions or interface formation strategies on multi-tissue scaffold designs (*bone-interface-ligament-interface-bone*, *tendon-interface-bone*, *muscle-interface-tendon* and *cartilage-interface-bone*) is a prerequisite for achieving graft integration and physiologic function. In addition, regional scaffold cues and cellular interactions can be used to direct cell fate in the absence of differentiation media either *in vitro* or *in vivo*. Specifically, spatial patterning of relevant key factors have been shown to exercise spatial control in stem cell differentiation on stratified and gradient scaffolds in which all regions are bathed in a common media.<sup>15,16,30,65,92,139</sup> Furthermore, heterotypic cellular interactions have been reported to ensure phenotypic maintenance and matrix integrity between zonal chondrocytes.<sup>48</sup> It is likely that spatial control of cell distribution and relevant inductive agents on the stratified or gradient scaffold is required to control the fate of each cell population and direct region-specific matrix elaboration. Moreover, it is noted that design requirements vary by tissue type and must take into consideration existing surgical practices for soft tissue repair. For example, while multi-tissue units are necessary for ligament reconstruction, scaffolds that can support non-calcified and calcified interface formation are sufficient for achieving functional tendon-bone integration. In contrast, calcified cartilage formation

alone is not sufficient for functional repair of a cartilage defect. Most importantly, for multi-tissue formation, the complex scaffold must exert spatial control over heterotypic cell interactions through incorporation of spatial and/or temporal compositional and chemical gradients, as well as through the use of biochemical and biomechanical stimulation to support the formation of integrated composite-tissue systems. Furthermore, scaffolds which support *in vivo* cellular infiltration and stem cell homing represent a promising future direction in the field as they have the potential to minimize the need to obtain, expand, and seed cells onto the scaffold prior to implantation. This approach will ultimately simplify the pathway to clinical translation and improve accessibility. The studies highlighted herein also demonstrate that functional and integrative connective tissue repair may be achieved by coupling both scaffold- and cell-based approaches.

Despite the exciting advancements in scaffold design and fabrication made in a relatively short period, there remain a number of challenges in this fast-growing field. One of the technical challenges in *ex vivo* engineering of complex tissues resides in how to devise an optimal culturing media or loading regimen that ensures the phenotypic maintenance of multiple cell populations and the elaboration of related matrix. For example, Wang *et al.* investigated the effects of ascorbic acid and  $\beta$ -GP dose on human osteoblasts and ligament fibroblasts, and devised a co-culture media which maintained osteoblast function without inducing unwanted mineralization by fibroblasts.<sup>127</sup> To this end, the mechanistic effects of biological, chemical, and physical stimuli must be thoroughly evaluated to enable more refined and targeted scaffold design and graft fixation. In addition to *in vitro* culture challenges, there remains a need for a greater understanding of the structure–function relationships at the native tissue–tissue interfaces, as well as the mechanisms governing interface development and healing at these junctions. Furthermore, physiologically relevant *in vitro* and *in vivo* models are needed to evaluate the clinical potential of these designs.

The *strategic biomimicry* approach emphasized here, where scaffolds can be designed to recapitulate the key compositional and structural organization properties of the native interface, will be instrumental for reestablishment of integrated musculoskeletal tissue systems and restoring physiologic function. It is anticipated that these efforts will lead to the development of the next generation of functional fixation devices for orthopaedic repair, as well as augment the potential for clinical translation of tissue-engineered orthopaedic grafts. Moreover, by bridging distinct types of tissues, interface tissue engineering will be

instrumental towards engineering complex organs and total limb or joint regeneration.

## ACKNOWLEDGMENTS

This work was supported by the National Institutes of Health (R21-AR056459, R01-AR055280, AR059038), and the New York State Stem Cell ESSC Board (NYSTEM C029551).

## REFERENCES

- <sup>1</sup>Alhadlaq, A., and J. J. Mao. Tissue-engineered osteochondral constructs in the shape of an articular condyle. *J. Bone Joint Surg. Am.* 87:936–944, 2005.
- <sup>2</sup>Allan, K. S., R. M. Pilliar, J. Wang, M. D. Gryn timer, and R. A. Kandel. Formation of biphasic constructs containing cartilage with a calcified zone interface. *Tissue Eng.* 13:167–177, 2007.
- <sup>3</sup>Altman, G. H., R. L. Horan, P. Weitzel, and J. C. Richmond. The use of long-term bioresorbable scaffolds for anterior cruciate ligament repair. *J. Am. Acad. Orthop. Surg.* 16:177–187, 2008.
- <sup>4</sup>Atala, A., F. K. Kasper, and A. G. Mikos. Engineering complex tissues. *Sci. Transl. Med.* 4:160rv12, 2012.
- <sup>5</sup>Aviv-Gavriel, M., N. Garti, and H. Furedi-Milhofer. Preparation of a partially calcified gelatin membrane as a model for a soft-to-hard tissue interface. *Langmuir* 29:683–689, 2013.
- <sup>6</sup>Aydin, H. M. A three-layered osteochondral plug: structural, mechanical, and *in vitro* biocompatibility analysis. *Adv. Eng. Mater.* 13:B511–B517, 2011.
- <sup>7</sup>Benjamin, M., E. J. Evans, and L. Copp. The histology of tendon attachments to bone in man. *J. Anat.* 149:89–100, 1986.
- <sup>8</sup>Benjamin, M., H. Toumi, J. R. Ralphs, G. Bydder, T. M. Best, and S. Milz. Where tendons and ligaments meet bone: attachment sites (‘entheses’) in relation to exercise and/or mechanical load. *J. Anat.* 208:471–490, 2006.
- <sup>9</sup>Bernstein, A., P. Niemeyer, G. Salzm ann, N. P. Sudkamp, R. Hube, J. Klehm, M. Menzel, R. von Eisenhart-Rothe, M. Bohner, L. Gorz, and H. O. Mayr. Microporous calcium phosphate ceramics as tissue engineering scaffolds for the repair of osteochondral defects: histological results. *Acta Biomater.* 9:7490–7505, 2013.
- <sup>10</sup>Blevins, F. T., M. Djurasovic, E. L. Flatow, and K. G. Vogel. Biology of the rotator cuff tendon. *Orthop. Clin. N. Am.* 28:1–16, 1997.
- <sup>11</sup>Bourke, S. L., J. Kohn, and M. G. Dunn. Preliminary development of a novel resorbable synthetic polymer fiber scaffold for anterior cruciate ligament reconstruction. *Tissue Eng.* 10:43–52, 2004.
- <sup>12</sup>Bullough, P. G., and A. Jagannath. The morphology of the calcification front in articular cartilage. Its significance in joint function. *J. Bone Jt. Surg. Br.* 65:72–78, 1983.
- <sup>13</sup>Castro, N. J., C. M. O’Brien, and L. G. Zhang. Biomimetic biphasic 3-D nanocomposite scaffold for osteochondral regeneration. *AIChE J.* 60:432–442, 2014.

- <sup>14</sup>Chang, C. H., C. H. Chen, C. Y. Su, H. T. Liu, and C. M. Yu. Rotator cuff repair with periosteum for enhancing tendon-bone healing: a biomechanical and histological study in rabbits. *Knee Surg. Sports Traumatol. Arthrosc.* 17:1447–1453, 2009.
- <sup>15</sup>Chen, J., H. Chen, P. Li, H. Diao, S. Zhu, L. Dong, R. Wang, T. Guo, J. Zhao, and J. Zhang. Simultaneous regeneration of articular cartilage and subchondral bone *in vivo* using MSCs induced by a spatially controlled gene delivery system in bilayered integrated scaffolds. *Biomaterials* 32:4793–4805, 2011.
- <sup>16</sup>Chen, G., T. Sato, J. Tanaka, and T. Tateishi. Preparation of a biphasic scaffold for osteochondral tissue engineering. *Mater. Sci. Eng. C* 26:118–123, 2006.
- <sup>17</sup>Cheng, H. W., K. D. Luk, K. M. Cheung, and B. P. Chan. *In vitro* generation of an osteochondral interface from mesenchymal stem cell-collagen microspheres. *Biomaterials* 32:1526–1535, 2011.
- <sup>18</sup>Chiang, H., C. J. Liao, C. H. Hsieh, C. Y. Shen, Y. Y. Huang, and C. C. Jiang. Clinical feasibility of a novel biphasic osteochondral composite for matrix-associated autologous chondrocyte implantation. *Osteoarthritis Cartilage* 21:589–598, 2013.
- <sup>19</sup>Cooper, J. A., H. H. Lu, F. K. Ko, J. W. Freeman, and C. T. Laurencin. Fiber-based tissue-engineered scaffold for ligament replacement: design considerations and *in vitro* evaluation. *Biomaterials* 26:1523–1532, 2005.
- <sup>20</sup>Cooper, R. R., and S. Misol. Tendon and ligament insertion. A light and electron microscopic study. *J. Bone Joint Surg. Am.* 52:1–20, 1970.
- <sup>21</sup>Cooper, Jr., J. A., J. S. Sahota, W. J. Gorum, J. Carter, S. B. Doty, and C. T. Laurencin. Biomimetic tissue-engineered anterior cruciate ligament replacement. *Proc. Natl. Acad. Sci. U.S.A.* 104:3049–3054, 2007.
- <sup>22</sup>Cui, W., X. Li, J. Chen, S. Zhou, and J. Weng. *In situ* growth kinetics of hydroxyapatite on electrospun poly(DL-lactide) fibers with gelatin grafted. *Cryst. Res. Technol.* 8:4576–4582, 2008.
- <sup>23</sup>Cui, W., X. Li, C. Xie, H. Zhuang, S. Zhou, and J. Weng. Hydroxyapatite nucleation and growth mechanism on electrospun fibers functionalized with different chemical groups and their combinations. *Biomaterials* 31:4620–4629, 2010.
- <sup>24</sup>Dickerson, D. A., T. N. Misk, S. Van, G. J. Breur, and E. A. Nauman. *In vitro* and *in vivo* evaluation of orthopedic interface repair using a tissue scaffold with a continuous hard tissue-soft tissue transition. *J. Orthop. Surg. Res.* 8:18, 2013.
- <sup>25</sup>Ding, C. M., Z. G. Qiao, W. B. Jiang, H. W. Li, J. H. Wei, G. D. Zhou, and K. R. Dai. Regeneration of a goat femoral head using a tissue-specific, biphasic scaffold fabricated with CAD/CAM technology. *Biomaterials* 34:6706–6716, 2013.
- <sup>26</sup>Dormer, N. H., M. Singh, L. Wang, C. J. Berkland, and M. S. Detamore. Osteochondral interface tissue engineering using macroscopic gradients of bioactive signals. *Ann. Biomed. Eng.* 38:2167–2182, 2010.
- <sup>27</sup>Dormer, N. H., M. Singh, L. Zhao, N. Mohan, C. J. Berkland, and M. S. Detamore. Osteochondral interface regeneration of the rabbit knee with macroscopic gradients of bioactive signals. *J. Biomed. Mater. Res. A* 100:162–170, 2012.
- <sup>28</sup>Dvir, T., B. P. Timko, D. S. Kohane, and R. Langer. Nanotechnological strategies for engineering complex tissues. *Nat. Nanotechnol.* 6:13–22, 2011.
- <sup>29</sup>Eriskin, C., D. M. Kalyon, and H. Wang. Functionally graded electrospun polycaprolactone and beta-tricalcium phosphate nanocomposites for tissue engineering applications. *Biomaterials* 29:4065–4073, 2008.
- <sup>30</sup>Eriskin, C., D. M. Kalyon, H. J. Wang, C. Ornek-Balanco, and J. H. Xu. Osteochondral tissue formation through adipose-derived stromal cell differentiation on biomimetic polycaprolactone nanofibrous scaffolds with graded insulin and beta-glycerophosphate concentrations. *Tissue Eng. Part A* 17:1239–1252, 2011.
- <sup>31</sup>Galatz, L. M., C. M. Ball, S. A. Teefey, W. D. Middleton, and K. Yamaguchi. The outcome and repair integrity of completely arthroscopically repaired large and massive rotator cuff tears. *J. Bone Jt. Surg. Am.* 86-A:219–224, 2004.
- <sup>32</sup>Galperin, A., R. A. Oldinski, S. J. Florczyk, J. D. Bryers, M. Q. Zhang, and B. D. Ratner. Integrated bi-Layered scaffold for osteochondral tissue engineering. *Adv. Healthcare Mater.* 2:872–883, 2013.
- <sup>33</sup>Gao, J., J. E. Dennis, L. A. Solchaga, A. S. Awadallah, V. M. Goldberg, and A. I. Caplan. Tissue-engineered fabrication of an osteochondral composite graft using rat bone marrow-derived mesenchymal stem cells. *Tissue Eng.* 7:363–371, 2001.
- <sup>34</sup>Genin, G. M., A. Kent, V. Birman, B. Wopenka, J. D. Pasteris, P. J. Marquez, and S. Thomopoulos. Functional grading of mineral and collagen in the attachment of tendon to bone. *Biophys. J.* 97:976–985, 2009.
- <sup>35</sup>Getelman, M. H., and M. J. Friedman. Revision anterior cruciate ligament reconstruction surgery. *J. Am. Acad. Orthop. Surg.* 7:189–198, 1999.
- <sup>36</sup>Getgood, A. M., S. J. Kew, R. Brooks, H. Aberman, T. Simon, A. K. Lynn, and N. Rushton. Evaluation of early-stage osteochondral defect repair using a biphasic scaffold based on a collagen-glycosaminoglycan biopolymer in a caprine model. *Knee* 19:422–430, 2012.
- <sup>37</sup>Grayson, W. L., S. Bhumiratana, P. H. Grace Chao, C. T. Hung, and G. Vunjak-Novakovic. Spatial regulation of human mesenchymal stem cell differentiation in engineered osteochondral constructs: effects of pre-differentiation, soluble factors and medium perfusion. *Osteoarthritis Cartilage* 18:714–723, 2010.
- <sup>38</sup>Harley, B. A., A. K. Lynn, Z. Wissner-Gross, W. Bonfield, I. V. Yannas, and L. J. Gibson. Design of a multiphase osteochondral scaffold III: Fabrication of layered scaffolds with continuous interfaces. *J. Biomed. Mater. Res. A* 92:1078–1093, 2010.
- <sup>39</sup>Harley, B. A., A. K. Lynn, Z. Wissner-Gross, W. Bonfield, I. V. Yannas, and L. J. Gibson. Design of a multiphase osteochondral scaffold III: Fabrication of layered scaffolds with continuous interfaces. *J. Biomed. Mater. Res. A* 92:1078–1093, 2010.
- <sup>40</sup>Hems, T., and B. Tillmann. Tendon entheses of the human masticatory muscles. *Anat. Embryol.* 202:201–208, 2000.
- <sup>41</sup>Heymer, A., G. Bradica, J. Eulert, and U. Noth. Multiphase collagen fibre-PLA composites seeded with human mesenchymal stem cells for osteochondral defect repair: an *in vitro* study. *J. Tissue Eng. Regen. Med.* 3:389–397, 2009.
- <sup>42</sup>Horan, R. L., I. Toponarski, H. E. Boepple, P. P. Weitzel, J. C. Richmond, and G. H. Altman. Design and characterization of a scaffold for anterior cruciate ligament engineering. *J. Knee Surg.* 22:82–92, 2009.
- <sup>43</sup>Huang, C. Y., V. M. Wang, R. J. Pawluk, J. S. Bucchieri, W. N. Levine, L. U. Bigliani, V. C. Mow, and E. L.



- Flatow. Inhomogeneous mechanical behavior of the human supraspinatus tendon under uniaxial loading. *J. Orthop. Res.* 23:924–930, 2005.
- <sup>44</sup>Hunziker, E. B. Articular cartilage repair: basic science and clinical progress. A review of the current status and prospects. *Osteoarthr. Cartilage* 10:432–463, 2002.
  - <sup>45</sup>Hunziker, E. B., I. M. Driesang, and C. Saager. Structural barrier principle for growth factor-based articular cartilage repair. *Clin. Orthop. Relat. Res.* 391:S182–S189, 2001.
  - <sup>46</sup>Hutmacher, D. W. Scaffolds in tissue engineering bone and cartilage. *Biomaterials* 21:2529–2543, 2000.
  - <sup>47</sup>Ibrahim, N. S., G. Krishnamurthy, H. R. B. Raghavendran, S. Puvaneswary, N. W. Min, and T. Kamarul. Novel HA-PVA/NOCC bilayered scaffold for osteochondral tissue-engineering applications—fabrication, characterization, *in vitro* and *in vivo* biocompatibility study. *Mater. Lett.* 113:25–29, 2013.
  - <sup>48</sup>Jiang, J., N. L. Leong, J. C. Mung, C. Hidaka, and H. H. Lu. Interaction between zonal populations of articular chondrocytes suppresses chondrocyte mineralization and this process is mediated by PTHrP. *Osteoarthr. Cartilage* 16:70–82, 2008.
  - <sup>49</sup>Jiang, J., A. Tang, G. A. Ateshian, X. E. Guo, C. T. Hung, and H. H. Lu. Bioactive stratified polymer ceramic-hydrogel scaffold for integrative osteochondral repair. *Ann. Biomed. Eng.* 38:2183–2196, 2010.
  - <sup>50</sup>Kandel, R. A., M. Hurtig, and M. Grynblas. Characterization of the mineral in calcified articular cartilaginous tissue formed *in vitro*. *Tissue Eng.* 5:25–34, 1999.
  - <sup>51</sup>Khanarian, N. T., M. K. Boushell, J. P. Spalazzi, N. Pleshko, A. L. Boskey, and H. H. Lu. FTIR-I compositional mapping of the cartilage-to-bone interface as a function of tissue region and age. *J. Bone Miner. Res.* 2014. doi:10.1002/jbmr.2284.
  - <sup>52</sup>Khanarian, N. T., N. M. Haney, R. A. Burga, and H. H. Lu. A functional agarose-hydroxyapatite scaffold for osteochondral interface regeneration. *Biomaterials* 33:5247–5258, 2012.
  - <sup>53</sup>Khanarian, N. T., J. Jiang, L. Q. Wan, V. C. Mow, and H. H. Lu. A hydrogel-mineral composite scaffold for osteochondral interface tissue engineering. *Tissue Eng. Part A* 18:533–545, 2012.
  - <sup>54</sup>Kimura, Y., A. Hokugo, T. Takamoto, Y. Tabata, and H. Kurosawa. Regeneration of anterior cruciate ligament by biodegradable scaffold combined with local controlled release of basic fibroblast growth factor and collagen wrapping. *Tissue Eng. Part C* 14:47–57, 2008.
  - <sup>55</sup>Kon, E., M. Delcogliano, G. Filardo, M. Busacca, M. A. Di, and M. Marcacci. Novel nano-composite multilayered biomaterial for osteochondral regeneration: a pilot clinical trial. *Am. J. Sports Med.* 39:1180–1190, 2011.
  - <sup>56</sup>Kon, E., A. Mutini, E. Arcangeli, M. Delcogliano, G. Filardo, A. N. Nicoli, D. Pressato, R. Quarto, S. Zaffagnini, and M. Marcacci. Novel nanostructured scaffold for osteochondral regeneration: pilot study in horses. *J. Tissue Eng. Regen. Med.* 4:300–308, 2010.
  - <sup>57</sup>Kostrominova, T. Y., S. Calve, E. M. Arruda, and L. M. Larkin. Ultrastructure of myotendinous junctions in tendon-skeletal muscle constructs engineered *in vitro*. *Histol. Histopathol.* 24:541–550, 2009.
  - <sup>58</sup>Ladd, M. R., S. J. Lee, J. D. Stitzel, A. Atala, and J. J. Yoo. Co-electrospun dual scaffolding system with potential for muscle-tendon junction tissue engineering. *Biomaterials* 32:1549–1559, 2011.
  - <sup>59</sup>Langer, R., and J. P. Vacanti. Tissue engineering. *Science* 260:920–926, 1993.
  - <sup>60</sup>Larkin, L. M., S. Calve, T. Y. Kostrominova, and E. M. Arruda. Structure and functional evaluation of tendon-skeletal muscle constructs engineered *in vitro*. *Tissue Eng.* 12:3149–3158, 2006.
  - <sup>61</sup>Laurencin, C. T., A. M. A. Ambrosio, M. D. Borden, and J. A. Cooper. Tissue engineering: orthopedic applications. *Annu. Rev. Biomed. Eng.* 1:19–46, 1999.
  - <sup>62</sup>Lee, J., W. Il Choi, G. Tae, Y. H. Kim, S. S. Kang, S. E. Kim, S. H. Kim, Y. Jung, and S. H. Kim. Enhanced regeneration of the ligament-bone interface using a poly(L-lactide-co-epsilon-caprolactone) scaffold with local delivery of cells/BMP-2 using a heparin-based hydrogel. *Acta Biomater.* 7:244–257, 2011.
  - <sup>63</sup>Li, Y., C. Ortiz, and M. C. Boyce. Stiffness and strength of suture joints in nature. *Phys. Rev. E* 84:062904, 2011.
  - <sup>64</sup>Li, X. R., J. W. Xie, J. Lipner, X. Y. Yuan, S. Thomopoulos, and Y. N. Xia. Nanofiber scaffolds with gradations in mineral content for mimicking the tendon-to-bone insertion site. *Nano Lett.* 9:2763–2768, 2009.
  - <sup>65</sup>Liu, W., J. Lipner, J. Xie, C. N. Manning, S. Thomopoulos, and Y. Xia. Nanofiber scaffolds with gradients in mineral content for spatial control of osteogenesis. *ACS Appl. Mater. Interfaces* 6:2842–2849, 2014.
  - <sup>66</sup>Liu, Y. X., S. Thomopoulos, V. Birman, J. S. Li, and G. M. Genin. Bi-material attachment through a compliant interfacial system at the tendon-to-bone insertion site. *Mech. Mater.* 44:83–92, 2012.
  - <sup>67</sup>Liu, W., Y. C. Yeh, J. Lipner, J. Xie, H. W. Sung, S. Thomopoulos, and Y. Xia. Enhancing the stiffness of electrospun nanofiber scaffolds with a controlled surface coating and mineralization. *Langmuir* 27:9088–9093, 2011.
  - <sup>68</sup>Lu, H. H., J. A. Cooper, Jr., S. Manuel, J. W. Freeman, M. A. Attawia, F. K. Ko, and C. T. Laurencin. Anterior cruciate ligament regeneration using braided biodegradable scaffolds: *in vitro* optimization studies. *Biomaterials* 26:4805–4816, 2005.
  - <sup>69</sup>Lu, H. H., J. Jiang, A. Tang, C. T. Hung, and X. E. Guo. Development of controlled heterogeneity on a polymer-ceramic hydrogel scaffold for osteochondral repair. *Biomaterials* 17:607–610, 2005.
  - <sup>70</sup>Lu, H. H., and S. Thomopoulos. Functional attachment of soft tissues to bone: development, healing, and tissue engineering. *Annu. Rev. Biomed. Eng.* 15:201–226, 2013.
  - <sup>71</sup>Ma, J., K. Goble, M. Smietana, T. Kostrominova, L. Larkin, and E. M. Arruda. Morphological and functional characteristics of three-dimensional engineered bone-ligament-bone constructs following implantation. *J. Biomech. Eng.* 131:101017, 2009.
  - <sup>72</sup>Ma, J., M. J. Smietana, T. Y. Kostrominova, E. M. Wojtyls, L. M. Larkin, and E. M. Arruda. Three-dimensional engineered bone-ligament-bone constructs for anterior cruciate ligament replacement. *Tissue Eng. Part A* 18:103–116, 2012.
  - <sup>73</sup>Mann, K. A., D. C. Ayers, F. W. Werner, R. J. Nicoletta, and M. D. Fortino. Tensile strength of the cement-bone interface depends on the amount of bone interdigitated with PMMA cement. *J. Biomech.* 30:339–346, 1997.
  - <sup>74</sup>Marquass, B., J. S. Somerson, P. Hepp, T. Aigner, S. Schwan, A. Bader, C. Josten, M. Zscharnack, and R. M. Schulz. A novel MSC-seeded triphasic construct for the repair of osteochondral defects. *J. Orthop. Res.* 28:1586–1599, 2010.

- <sup>75</sup>Matyas, J. R., M. G. Anton, N. G. Shrive, and C. B. Frank. Stress governs tissue phenotype at the femoral insertion of the rabbit MCL. *J. Biomech.* 28:147–157, 1995.
- <sup>76</sup>Mente, P. L., and J. L. Lewis. Elastic modulus of calcified cartilage is an order of magnitude less than that of subchondral bone. *J. Orthop. Res.* 12:637–647, 1994.
- <sup>77</sup>Mikos, A. G., S. W. Herring, P. Ochareon, J. Elisseeff, H. H. Lu, R. Kandel, F. J. Schoen, M. Toner, D. Mooney, A. Atala, M. E. Dyke, D. Kaplan, and G. Vunjak-Novakovic. Engineering complex tissues. *Tissue Eng.* 12:3307–3339, 2006.
- <sup>78</sup>Moffat, K. L., R. T. Cassilly, S. D. Subramony, *et al.* In vivo evaluation of a bi-phasic nanofiber-based scaffold for integrative rotator cuff repair. In: Transactions of the 56th Orthopaedic Research Society, 2010.
- <sup>79</sup>Moffat, K. L., W. N. Levine, and H. H. Lu. In vitro evaluation of rotator cuff tendon fibroblasts on aligned composite scaffold of polymer nanofibers and hydroxyapatite nanoparticles. In: Transactions of the 54th Orthopaedic Research Society, 2008.
- <sup>80</sup>Moffat, K. L., W. H. Sun, P. E. Pena, N. O. Chahine, S. B. Doty, G. A. Ateshian, C. T. Hung, and H. H. Lu. Characterization of the structure-function relationship at the ligament-to-bone interface. *Proc. Natl. Acad. Sci. U.S.A.* 105:7947–7952, 2008.
- <sup>81</sup>Mohan, N., N. H. Dormer, K. L. Caldwell, V. H. Key, C. J. Berkland, and M. S. Detamore. Continuous gradients of material composition and growth factors for effective regeneration of the osteochondral interface. *Tissue Eng. Part A* 17:2845–2855, 2011.
- <sup>82</sup>Mohan, N., V. Gupta, B. Sridharan, A. Sutherland, and M. S. Detamore. The potential of encapsulating “raw materials” in 3D osteochondral gradient scaffolds. *Biotechnol. Bioeng.* 111:829–841, 2014.
- <sup>83</sup>Myers, B. S., C. T. Woolley, T. L. Slotter, W. E. Garrett, and T. M. Best. The influence of strain rate on the passive and stimulated engineering stress–large strain behavior of the rabbit tibialis anterior muscle. *J. Biomech. Eng.* 120:126–132, 1998.
- <sup>84</sup>Oegema, Jr., T. R., R. J. Carpenter, F. Hofmeister, and R. C. Thompson, Jr. The interaction of the zone of calcified cartilage and subchondral bone in osteoarthritis. *Microsc. Res. Tech.* 37:324–332, 1997.
- <sup>85</sup>Oegema Jr., T. R., and R. C. Thompson Jr. Cartilage-bone interface (tidemark). In: *Cartilage Changes in Osteoarthritis*, edited by K. D. Brandt. Indianapolis, IN: Indiana School of Medicine Publication, 1990, pp. 43–52.
- <sup>86</sup>Paxton, J. Z., K. Donnelly, R. P. Keatch, and K. Baar. Engineering the bone-ligament interface using polyethylene glycol diacrylate incorporated with hydroxyapatite. *Tissue Eng. Part A* 15:1201–1209, 2009.
- <sup>87</sup>Paxton, J. Z., L. M. Grover, and K. Baar. Engineering an in vitro model of a functional ligament from bone to bone. *Tissue Eng. Part A* 16(11):3515–3525, 2010.
- <sup>88</sup>Phillips, J. E., K. L. Burns, J. M. Le Doux, R. E. Guldberg, and A. J. Garcia. Engineering graded tissue interfaces. *Proc. Natl. Acad. Sci. U.S.A.* 105:12170–12175, 2008.
- <sup>89</sup>Qu, D., S. D. Subramony, A. L. Boskey, *et al.* Compositional mapping of the mature anterior cruciate ligament-to-bone insertion site. In: Transactions of the Orthopaedic Research Society, 2014.
- <sup>90</sup>Quain, J. *Elements of Anatomy*. In 3 Volumes. New York, NY: Walton and Maberly, 1856.
- <sup>91</sup>Redler, I., V. C. Mow, M. L. Zimny, and J. Mansell. The ultrastructure and biomechanical significance of the tide-mark of articular cartilage. *Clin. Orthop. Relat. Res.* 112:357–362, 1975.
- <sup>92</sup>Re'em, T., F. Witte, E. Willbold, E. Ruvinov, and S. Cohen. Simultaneous regeneration of articular cartilage and subchondral bone induced by spatially presented TGF-beta and BMP-4 in a bilayer affinity binding system. *Acta Biomater.* 8:3283–3293, 2012.
- <sup>93</sup>Rodeo, S. A., S. P. Arnoczky, P. A. Torzilli, C. Hidaka, and R. F. Warren. Tendon-healing in a bone tunnel. A biomechanical and histological study in the dog. *J. Bone Jt. Surg. Am.* 75:1795–1803, 1993.
- <sup>94</sup>Rumian, A. P., A. L. Wallace, and H. L. Birch. Tendons and ligaments are anatomically distinct but overlap in molecular and morphological features—a comparative study in an ovine model. *J. Orthop. Res.* 25:458–464, 2007.
- <sup>95</sup>Salerno, A., S. Iannace, and P. A. Netti. Graded biomimetic osteochondral scaffold prepared via CO<sub>2</sub> foaming and micronized NaCl leaching. *Mater. Lett.* 82:137–140, 2012.
- <sup>96</sup>Samavedi, S., S. A. Guelcher, A. S. Goldstein, and A. R. Whittington. Response of bone marrow stromal cells to graded co-electrospun scaffolds and its implications for engineering the ligament-bone interface. *Biomaterials* 33:7727–7735, 2012.
- <sup>97</sup>Samavedi, S., C. Olsen Horton, S. A. Guelcher, A. S. Goldstein, and A. R. Whittington. Fabrication of a model continuously graded co-electrospun mesh for regeneration of the ligament-bone interface. *Acta Biomater.* 7:4131–4138, 2011.
- <sup>98</sup>Samavedi, S., P. Vaidya, P. Gaddam, A. R. Whittington, and A. S. Goldstein. Electrospun meshes possessing region-wise differences in fiber orientation, diameter, chemistry and mechanical properties for engineering bone-ligament-bone tissues. *Biotechnol. Bioeng.* 111(12): 2549–2559, 2014.
- <sup>99</sup>Sano, H., Y. Saijo, and S. Kokubun. Non-mineralized fibrocartilage shows the lowest elastic modulus in the rabbit supraspinatus tendon insertion: measurement with scanning acoustic microscopy. *J. Shoulder Elbow Surg.* 15:743–749, 2006.
- <sup>100</sup>Schaefer, D., I. Martin, P. Shastri, R. F. Padera, R. Langer, L. E. Freed, and G. Vunjak-Novakovic. In vitro generation of osteochondral composites. *Biomaterials* 21:2599–2606, 2000.
- <sup>101</sup>Scotti, C., D. Wirz, F. Wolf, D. J. Schaefer, V. Burgin, A. U. Daniels, V. Valderrabano, C. Candrian, M. Jakob, I. Martin, and A. Barbero. Engineering human cell-based, functionally integrated osteochondral grafts by biological bonding of engineered cartilage tissues to bony scaffolds. *Biomaterials* 31:2252–2259, 2010.
- <sup>102</sup>Seo, J. P., T. Tanabe, N. Tsuzuki, S. Haneda, K. Yamada, H. Furuoka, Y. Tabata, and N. Sasaki. Effects of bilayer gelatin/beta-tricalcium phosphate sponges loaded with mesenchymal stem cells, chondrocytes, bone morphogenetic protein-2, and platelet rich plasma on osteochondral defects of the talus in horses. *Res. Vet. Sci.* 95:1210–1216, 2013.
- <sup>103</sup>Shao, X., J. C. Goh, D. W. Huttmacher, E. H. Lee, and G. Zigang. Repair of large articular osteochondral defects using hybrid scaffolds and bone marrow-derived mesenchymal stem cells in a rabbit model. *Tissue Eng.* 12:1539–1551, 2006.

- <sup>104</sup>Sherwood, J. K., S. L. Riley, R. Palazzolo, S. C. Brown, D. C. Monkhouse, M. Coates, L. G. Griffith, L. K. Landeen, and A. Ratcliffe. A three-dimensional osteochondral composite scaffold for articular cartilage repair. *Biomaterials* 23:4739–4751, 2002.
- <sup>105</sup>Shi, J., L. Wang, F. Zhang, H. Li, L. Lei, L. Liu, and Y. Chen. Incorporating protein gradient into electrospun nanofibers as scaffolds for tissue engineering. *ACS Appl. Mater. Interfaces* 2:1025–1030, 2010.
- <sup>106</sup>Singh, M., N. Dormer, J. R. Salash, J. M. Christian, D. S. Moore, C. Berkland, and M. S. Detamore. Three-dimensional macroscopic scaffolds with a gradient in stiffness for functional regeneration of interfacial tissues. *J. Biomed. Mater. Res. A* 94:870–876, 2010.
- <sup>107</sup>Skalak, R. Tissue Engineering: Proceedings of a Workshop, Held at Granlibakken, Lake Tahoe, California, February 26–29, 1988; New York, NY: Liss, 1988.
- <sup>108</sup>Soltz, M. A., and G. A. Ateshian. Experimental verification and theoretical prediction of cartilage interstitial fluid pressurization at an impermeable contact interface in confined compression. *J. Biomech.* 31:927–934, 1998.
- <sup>109</sup>Spalazzi, J. P., A. L. Boskey, N. Pleshko, and H. H. Lu. Quantitative mapping of matrix content and distribution across the ligament-to-bone insertion. *PLoS ONE* 8:e74349, 2013.
- <sup>110</sup>Spalazzi, J. P., E. Dagher, S. B. Doty, X. E. Guo, S. A. Rodeo, and H. H. Lu. *In vivo* evaluation of a multiphased scaffold designed for orthopaedic interface tissue engineering and soft tissue-to-bone integration. *J. Biomed. Mater. Res. A* 86:1–12, 2008.
- <sup>111</sup>Spalazzi, J. P., S. B. Doty, K. L. Moffat, W. N. Levine, and H. H. Lu. Development of controlled matrix heterogeneity on a triphasic scaffold for orthopedic interface tissue engineering. *Tissue Eng.* 12:3497–3508, 2006.
- <sup>112</sup>Spalazzi, J. P., J. Gallina, S. D. Fung-Kee-Fung, E. E. Konofagou, and H. H. Lu. Elastographic imaging of strain distribution in the anterior cruciate ligament and at the ligament-bone insertions. *J. Orthop. Res.* 24:2001–2010, 2006.
- <sup>113</sup>Spalazzi, J. P., M. C. Vyner, M. T. Jacobs, K. L. Moffat, and H. H. Lu. Mechanoactive scaffold induces tendon remodeling and expression of fibrocartilage markers. *Clin. Orthop. Relat. Res.* 466:1938–1948, 2008.
- <sup>114</sup>Subramony, S. D., D. Delos, A. Weber, et al. *In vivo* evaluation of a mechanoactive nanofiber scaffold for integrative ACL reconstruction. In: Transactions of the 57th Orthopaedic Research Society, 2011.
- <sup>115</sup>Subramony, S. D., D. Qu, R. Ma, et al. *In vitro* optimization and *in vivo* evaluation of a multi-phased nanofiber-based synthetic ACL scaffold. In: Transactions of the 60th Orthopaedic Research Society, 2014.
- <sup>116</sup>Sundar, S., C. J. Pendegrass, and G. W. Blunn. Tendon bone healing can be enhanced by demineralized bone matrix: a functional and histological study. *J. Biomed. Mater. Res. B* 88:115–122, 2009.
- <sup>117</sup>Swasdison, S., and R. Mayne. *In vitro* attachment of skeletal muscle fibers to a collagen gel duplicates the structure of the myotendinous junction. *Exp. Cell Res.* 193:227–231, 1991.
- <sup>118</sup>Swasdison, S., and R. Mayne. Formation of highly organized skeletal muscle fibers *in vitro*. Comparison with muscle development *in vivo*. *J. Cell Sci.* 102:643–652, 1992.
- <sup>119</sup>Swieszkowski, W., B. H. S. Tuan, K. J. Kurzydowski, and D. W. Hutmacher. Repair and regeneration of osteochondral defects in the articular joints. *Biomol. Eng.* 24:489–495, 2007.
- <sup>120</sup>Temenoff, J. S., and A. G. Mikos. Review: tissue engineering for regeneration of articular cartilage. *Biomaterials* 21:431–440, 2000.
- <sup>121</sup>Thomopoulos, S., G. R. Williams, J. A. Gimbel, M. Favata, and L. J. Soslowsky. Variations of biomechanical, structural, and compositional properties along the tendon to bone insertion site. *J. Orthop. Res.* 21:413–419, 2003.
- <sup>122</sup>Tidball, J. G. Myotendinous junction: morphological changes and mechanical failure associated with muscle cell atrophy. *Exp. Mol. Pathol.* 40:1–12, 1984.
- <sup>123</sup>Tidball, J. G. Myotendinous junction injury in relation to junction structure and molecular composition. *Exerc. Sport Sci. Rev.* 19:419–445, 1991.
- <sup>124</sup>Trotter, J. A. Structure-function considerations of muscle–tendon junctions. *Comp. Biochem. Physiol. A* 133:1127–1133, 2002.
- <sup>125</sup>Vunjak-Novakovic, G., G. Altman, R. Horan, and D. L. Kaplan. Tissue engineering of ligaments. *Annu. Rev. Biomed. Eng.* 6:131–156, 2004.
- <sup>126</sup>Wang, I. E., S. Mitroo, F. H. Chen, H. H. Lu, and S. B. Doty. Age-dependent changes in matrix composition and organization at the ligament-to-bone insertion. *J. Orthop. Res.* 24:1745–1755, 2006.
- <sup>127</sup>Wang, I. E., J. Shan, R. Choi, S. Oh, C. K. Kepler, F. H. Chen, and H. H. Lu. Role of osteoblast–fibroblast interactions in the formation of the ligament-to-bone interface. *J. Orthop. Res.* 25:1609–1620, 2007.
- <sup>128</sup>Wang, X., E. Wenk, X. Zhang, L. Meinel, G. Vunjak-Novakovic, and D. L. Kaplan. Growth factor gradients via microsphere delivery in biopolymer scaffolds for osteochondral tissue engineering. *J. Control Release* 134:81–90, 2009.
- <sup>129</sup>Weitzel, P. P., J. C. Richmond, G. H. Altman, T. Calabro, and D. L. Kaplan. Future direction of the treatment of ACL ruptures. *Orthop. Clin. N. Am.* 33:653–661, 2002.
- <sup>130</sup>Woo, S. L., J. Maynard, D. L. Butler, et al. Ligament, tendon, and joint capsule insertions to bone. In: *Injury and Repair of the Musculoskeletal Soft Tissues*, edited by S. L. Woo, and J. A. Buckwalter. Savannah, GA: American Academy of Orthopaedic Surgeons, 1988, pp. 133–166.
- <sup>131</sup>Wren, T. A., S. A. Yerby, G. S. Beaupre, and D. R. Carter. Mechanical properties of the human achilles tendon. *Clin. Biomech.* 16:245–251, 2001.
- <sup>132</sup>Yang, P. J., and J. S. Temenoff. Engineering orthopedic tissue interfaces. *Tissue Eng. Part B* 15:127–141, 2009.
- <sup>133</sup>Yunos, D., Z. Ahmad, V. Salih, and A. Boccaccini. Stratified scaffolds for osteochondral tissue engineering applications: electrospun PDLLA nanofibre coated Bioglass(R)-derived foams. *J. Biomater. Appl.* 27:537–551, 2013.
- <sup>134</sup>Zhang, X., J. M. Caldwell, J. Easley, et al. *In vivo* evaluation of a biomimetic biphasic scaffold in sheep. In: Transactions of the 60th Orthopaedic Research Society, 2014.
- <sup>135</sup>Zhang, S., L. Chen, Y. Jiang, Y. Cai, G. Xu, T. Tong, W. Zhang, L. Wang, J. Ji, P. Shi, and H. W. Ouyang. Bi-layer collagen/microporous electrospun nanofiber scaffold improves the osteochondral regeneration. *Acta Biomater.* 9:7236–7247, 2013.
- <sup>136</sup>Zhang, W., J. L. Chen, J. D. Tao, C. C. Hu, L. K. Chen, H. S. Zhao, G. W. Xu, B. C. Heng, and H. W. Ouyang. The promotion of osteochondral repair by combined intra-articular injection of parathyroid hormone-related protein and implantation of a bi-layer collagen-silk scaffold. *Biomaterials* 34:6046–6057, 2013.



- <sup>137</sup>Zhang, K., Y. Ma, and L. F. Francis. Porous polymer/bioactive glass composites for soft-to-hard tissue interfaces. *J. Biomed. Mater. Res.* 61:551–563, 2002.
- <sup>138</sup>Zhen, G., and X. Cao. Targeting TGFbeta signaling in subchondral bone and articular cartilage homeostasis. *Trends Pharmacol. Sci.* 35:227–236, 2014.
- <sup>139</sup>Zou, B., Y. Liu, X. Luo, F. Chen, X. Guo, and X. Li. Electrospun fibrous scaffolds with continuous gradations in mineral contents and biological cues for manipulating cellular behaviors. *Acta Biomater.* 8: 1576–1585, 2012.